Inorg. Chem. **2006**, *45*, 2008–2021

The Butterfly Dimer $[(^tBu_3SiO)Cr]_2(\mu\text{-}OSi^tBu_3)_2$ and Its Oxidative Cleavage to $(^tBu_3SiO)_2Cr(=N–N=CPh_2)_2$ and $(^tBu_3SiO)_2Cr=N(2,6\text{-}Ph_2\text{-}C_6H_3)$

Orson L. Sydora,[†] David S. Kuiper,[†] Peter T. Wolczanski,*[,†] Emil B. Lobkovsky,[†] Adriana Dinescu,[‡] and Thomas R. Cundari[‡]

Department of Chemistry and Chemical Biology, Baker Laboratory, Cornell University, Ithaca, New York 14853, and Department of Chemistry, University of North Texas, Box 305070, Denton, Texas 76203-5070

Received August 30, 2005

Treatment of $CrCl_2(THF)_2$ with $NaOSi^tBu_3$ afforded the butterfly dimer $[(^tBu_3SiO)Cr]_2(\mu\text{-}OSi^tBu_3)_2$ (**1**$_2$), whose *d*(CrCr) of 2.658(31) Å and magnetism were indicative of strong antiferromagnetic coupling. A Boltzmann distribution of low-energy $^1A_1$, $^3B_1$, $^5A_1$, $^7B_1$, and $^9A_1$ states obtained from calculations on $[(HO)_2Cr]_2(\mu OH)_2$ (**1′**$_2$) were used to provide a reasonable fit of the μ_{eff} vs *T* data. Cleavage of **1**$_2$ with various L (L = 4-picoline, *p*-tolunitrile, ^{t}BuCN, ^{t}BuNC, Ph_2CO, and PMe_3) generated $(^tBu_3SiO)_2CrL_2$ (**1**-L$_2$). The dimer was oxidatively severed by Ph_2CN_2 to give $(^tBu_3SiO)_2Cr(N_2CPh_2)_2$ (**2**) and by RN_3 at 23 °C to afford $(silox)_2Cr{=}NR$ (**3**-R) for bulky R (adamantyl (Ad), 2,6-$^iPr_2$–C_6H_3, 2,4,6-Me_3–C_6H_2 = Mes, 2,6-Ph_2-C_6H_3) and $(^tBu_3SiO)_2Cr(=NR)_2$ (**4**-R) for smaller substituents (R = 1-Naph, 2-Anth). X-ray structural studies were conducted on **1**$_2$, square planar **1**-$(OCPh_2)_2$, pseudo-T_d **2** and pseudo-trigonal **3**-(2,6-Ph_2-C_6H_3), whose $S = 1$ ground state was discussed on the basis of calculations of $(H_3SiO)_2Cr{=}NPh$ (**3′′**-Ph).

Introduction

The generation of electronically and coordinatively unsaturated transition metal fragments leaves them susceptible to aggregation, but through the use of bulky ligands, low-coordinate species can often be isolated. For example, the bulky siloxide $^tBu_3SiO^-$ (silox) has been successfully employed to stabilize low-coordinate mononuclear complexes such as $[(silox)_3M]^n$ ($n = 0$, M = Ti,[1] V, NbL (L = PMe_3, 4-picoline),[2] Ta;[3] $n = 1-$, M = Cr).[4] These compounds have been shown to be exceedingly reactive in CX bond activations,[5] displaying chemistry as diverse as carbon monoxide and related CO bond cleavages,[3,6] other deoxygenations,[2] olefin-to-alkylidene rearrangements,[7] and pyridine ring-openings.[8,9] In these systems, a severe steric price is paid in order to observe such dramatic reactivity, often limiting the chemistry to small molecules. In addition, the silox ligands can become directly involved.[7,10]

Another means of utilizing features of low-valent metal centers in bond activations is via the creation of metal−metal-bonded complexes that can exhibit substantial reactivity through reactions at their metal−metal bonds.[11]

* To whom correspondence should be addressed. E-mail: ptw2@cornell.edu.

[†] Cornell University.

[‡] University of North Texas.

(1) Covert, K. J.; Wolczanski, P. T.; Hill, S. A.; Krusic, P. J. *Inorg. Chem.* **1992**, *31*, 66−78.

(2) Veige, A. S.; Slaughter, L. M.; Lobkovsky, E. B.; Wolczanski, P. T.; Matsunaga, N.; Decker, S. A.; Cundari, T. R. *Inorg. Chem.* **2003**, *42*, 6204−6224.

(3) Neithamer, D. R.; LaPointe, R. E.; Wheeler, R. A.; Richeson, D. S.; Van Duyne, G. D.; Wolczanski, P. T. *J. Am. Chem. Soc.* **1989**, *111*, 9056−9072.

(4) Sydora, O. L.; Wolczanski, P. T.; Lobkovsky, E. B.; Buda, C.; Cundari, T. R. *Inorg. Chem.* **2005**, *44*, 2606−2618.

(5) Wolczanski, P. T. *Polyhedron* **1995**, *22*, 3335−3362.

(6) (a) Covert, K. J.; Mayol, A.-R.; Wolczanski, P. T. *Inorg. Chim. Acta.* **1997**, *263*, 263−278. (b) Veige, A. S.; Kleckley, T. S.; Chamberlin, R. L. M.; Neithamer, D. R.; Lee, C. E.; Wolczanski, P. T.; Lobkovsky, E. B.; Glassey, W. V., *J. Organomet. Chem.* **1999**, *591*, 194−203.

(7) (a) Hirsekorn, K. F.; Veige, A. S.; Marshak, M. P.; Koldobskaya, Y.; Wolczanski, P. T.; Cundari, T. R.; Lobkovsky, E. B. *J. Am. Chem. Soc.* **2005**, *127*, 4809−4830. (b) Veige, A. S.; Wolczanski, P. T.; Lobkovsky, E. B., *Angew. Chem., Int. Ed.* **2001**, *40*, 3629−3632.

(8) Kleckley, T. S.; Bennett, J. L.; Wolczanski, P. T.; Lobkovsky, E. B. *J. Am. Chem. Soc.* **1997**, *119*, 247−248.

(9) Bonanno, J. B.; Henry, T. P.; Neithamer, D. R.; Wolczanski, P. T.; Lobkovsky, E. B. *J. Am. Chem. Soc.* **1996**, *118*, 5132−5133.

(10) Bonanno, J. B.; Veige, A. S.; Wolczanski, P. T.; Lobkovsky, E. B. *Inorg. Chim. Acta* **2003**, *345*, 173−184.

(11) Cotton, F. A.; Walton, R. A. *Multiple Bonds Between Metal Atoms;* Oxford University Press: New York, 1993.

10.1021/ic051481w CCC: $33.50
Published on Web 01/12/2006

Table 1. Crystallographic Data for $[(^tBu_3SiO)Cr]_2(\mu\text{-}OSi^tBu_3)_2$ (**1**$_2$), *trans*-$(silox)_2Cr(O{=}CPh_2)_2$ (**1**-$(OCPh_2)_2$), $(silox)_2Cr(=N-N{=}CPh_2)_2$ (**2**), and $(silox)_2Cr{=}N(2,6\text{-}Ph_2\text{-}C_6H_3)$ (**3**-$(2,6\text{-}Ph_2\text{-}C_6H_3)$)

	1$_2$	**1**-$(OCPh_2)_2$	**2**	**3**-$(2,6\text{-}Ph_2\text{-}C_6H_3)$
formula	$C_{106}H_{240}O_8Si_8Cr_4$[a]	$C_{25}H_{37}O_2SiCr_{0.5}$[b]	$C_{55}H_{86}N_4O_2Si_2Cr$	$C_{42}H_{67}O_2NSi_2Cr$
fw	2075.76	423.67	943.50	726.17
space group	$Pna2_1$	$C2$	Pc	$P2_12_12_1$
Z	4	4	2	4
a, Å	24.524(5)	24.474(3)	12.7050(17)	13.0755(6)
b, Å	23.142(5)	9.4762(13)	18.890(3)	15.5264(6)
c, Å	22.978(5)	11.7561(13)	13.1447(18)	21.3870(11)
α, deg	90	90	90	90
β, deg	90	113.785(13)	116.852(3)	90
γ, deg	90	90	90	90
V, Å^3	13041(5)	2495.0(5)	2814.6(7)	4341.9(3)
ρ_{calc}, g·cm^{-3}	1.057	1.128	1.113	1.111
μ, mm^{-1}	0.443	0.317	0.286	0.351
temp, K	173(2)	173(2)	173(2)	173(2)
λ (Å)	0.71073	0.71073	0.71073	0.71073
R ind $[I > 2\sigma(I)]$[c,d]	R1 = 0.0654	R1 = 0.0632	R1 = 0.0449	R1 = 0.0413
	wR2 = 0.1467	wR2 = 0.1664	wR2 = 0.0906	wR2 = 0.1071
R ind (all data)[c,d]	R1 = 0.1201	R1 = 0.0767	R1 = 0.0660	R1 = 0.0565
	wR2 = 0.1803	wR2 = 0.1771	wR2 = 0.0989	wR2 = 0.1153
GOF[e]	1.014	1.244	0.979	0.960

[a] The asymmetric unit (formula) contains two molecules. [b] The asymmetric unit (formula) contains one-half of a molecule. [c] $R1 = \sum||F_o| - |F_c||/|F_o|$. [d] $wR2 = [\sum w(|F_o| - |F_c|)^2/\sum wF_o^2]^{1/2}$. [e] GOF (all data) $= [\sum w(|F_o| - |F_c|)^2/(n - p)]^{1/2}$, n = number of independent reflections, p = number of parameters.

The chemistry of group 6 triple-bonded complexes, $X_{3-n}Y_nMMX_{3-n}Y_n$, is dominated by direct involvement of the electron density comprising the M≡M unit, and encompasses a host of bond activations.[11,12] When $(silox)_nX_mM$ fragments form metal−metal multiple bonds, the resulting dimers can be remarkably inert (cf. $(silox)_2ORe{\equiv}ReO(silox)_2$),[13] or they can display intriguing small-molecule chemistry (e.g., $(silox)_2(CO)ClW{\equiv}WCl(CO)(silox)_2 \rightarrow (silox)_2OW{=}C{=}WCl_2(silox)_2 + CO$).[14] A previous report on the generation of "(silox)CrCl" revealed its aggregation to the chromous "box", $[(\mu\text{-}Cl)Cr(\mu\text{-}OSi^tBu_3)]_4$, and cleavage to afford $(silox)_3Cr^-$, among other species.[4] Reported herein is the chemistry of an unusual first-row dichromium complex, $[(^tBu_3SiO)Cr]_2(\mu\text{-}OSi^tBu_3)_2$, which reacts somewhat differently, because it can be simply rationalized as a source of "$(silox)_2Cr$".

Results and Discussion

$[(^tBu_3SiO)Cr]_2(\mu\text{-}OSi^tBu_3)_2$ (1$_2$). 1. Synthesis. Treatment of $CrCl_2(THF)_2$ with ∼1.5 equiv of $NaOSi^tBu_3$ in THF for 10 h afforded a green solid that was heated at 70 °C to remove residual solvent. Crystallization from pentane at −78 °C provided green blocks of $[(^tBu_3SiO)Cr]_2(\mu\text{-}OSi^tBu_3)_2$ (**1**$_2$) in 74% yield (eq 1). The use of less than a stoichiometric amount of sodium siloxide was necessary to avoid

$$CrCl_2(THF)_2 + 2NaOSi^tBu_3 \xrightarrow[70\ ^\circ C,\ -THF]{THF,\ 10\ h,\ 23\ ^\circ C} \underset{\mathbf{1}_2}{[(^tBu_3SiO)Cr]_2(\mu\text{-}OSi^tBu_3)_2} + 2NaCl \quad (1)$$

formation of $[(silox)_3Cr]Na(THF)_n$,[4] which interfered with the isolation of dimeric **1**$_2$. Two structures were considered for **1**$_2$: a D_{2d} quadruple-bonded $[(^tBu_3SiO)_2Cr]_2$ conformer,[15] and one possessing two bridging siloxides and two terminal siloxides. The ^{1}H NMR spectrum of **1**$_2$ was relatively uninformative (δ 1.71, $\nu_{1/2} \approx$ 210 Hz); thus, an X-ray structural examination of the dimer ensued.

2. Molecular Structure. Details of the data collection and refinement pertaining to **1**$_2$ are summarized in Table 1, and selected interatomic distances and angles are given in Table 2. The asymmetric unit contained two independent isostructural chromous dimers, each possessing two bridging and two terminal silox groups. Subtly different chromium−chromium distances of 2.6365(15) (Cr1−Cr2) and 2.6800(15) Å (Cr1′−Cr2′) prompted careful scrutiny of the structure solution to see if a centrosymmetric space group (e.g., *Pnma*) was more appropriate, but refinement in $Pna2_1$ proved best. Several crystals were tried in an attempt to provide better data, but none successfully refined better, and the space group was consistent. It is conceivable that weakly antiferromagnetically coupled chromous centers could be subject to minor distance deviations as a function of external (e.g., packing) forces; nonetheless, the distances are approximately equal and, while out of the realm of multiple-bonding interactions,[11] are plausible for a weak single bond ($r_{cov}(Cr) = 1.18$ Å).

1$_2$ may also be described as a butterfly dimer containing pseudo-trigonal chromous centers connected by the bridging siloxides, as Figure 1 reveals. The planes defined by the Cr-

(12) (a) Chisholm, M. H. *J. Chem. Soc., Dalton Trans.* **1996**, 1781−1791. (b) Chisholm, M. H. *J. Organomet. Chem.* **1990**, *400*, 235−253. (c) Chisholm, M. H. *Acc. Chem. Res.* **1990**, *23*, 419−425. (d) Buhro, W. E.; Chisholm, M. H. *Adv. Organomet. Chem.* **1987**, *27*, 311−369. (e) Chisholm, M. H.; Conroy, B. K.; Eichhorn, B. W.; Folting, K.; Hoffman, D. M.; Huffman, J. C.; Marchant, N. S. *Polyhedron* **1987**, *6*, 783−792. (f) Chisholm, M. H.; Hoffman, D. M.; Huffman, J. C. *Chem. Soc. Rev.* **1985**, *14*, 69−91.

(13) Douthwaite, R. E.; Wolczanski, P. T.; Merschrod, E. *J. Chem. Soc. Chem. Commun.* **1998**, 2591−2592.

(14) (a) Miller, R. L.; Wolczanski, P. T.; Rheingold, A. L. *J. Am. Chem. Soc.* **1993**, *115*, 10422−10423. (b) Miller, R. L.; Lawler, K. A.; Bennett, J. L.; Wolczanski, P. T. *Inorg. Chem.* **1996**, *35*, 3242−3253.

(15) Chamberlin, R. L. M.; Rosenfeld, D. C.; Wolczanski, P. T.; Lobkovsky, E. B. *Organometallics* **2002**, *21*, 2724−2735.

Table 2. Selected Interatomic Distances (Å) and Angles (deg) for [(^{t}Bu$_3$SiO)Cr]$_2$(μ-OSi^{t}Bu$_3$)$_2$ (**1**$_2$)

Cr1−O1	1.835(4)	Cr1−O3	2.006(4)	Cr1−O4	1.996(4)
Cr2−O2	1.870(4)	Cr2−O3	1.991(4)	Cr2−O4	1.980(4)
Cr1′−O1′	1.845(5)	Cr1′−O3′	2.013(4)	Cr1′−O4′	1.995(4)
Cr2′−O2′	1.870(4)	Cr2′−O3′	2.004(4)	Cr2′−O4′	1.984(4)
Si1−O1	1.640(5)	Si2−O2	1.629(5)	Si3−O3	1.670(4)
Si4−O4	1.670(4)	Si1′−O1′	1.626(5)	Si2′−O2′	1.637(5)
Si3′−O3′	1.663(4)	Si4′−O4′	1.677(4)	Si−C(ave)	1.929(13)
Cr1−Cr2	2.6365(15)	Cr1′-Cr2′	2.6800(15)	C−C(ave)	1.53(4)
O1−Cr1−O3	138.2(2)	O1−Cr1−O4	137.2(2)	O3−Cr1−O4	82.7(2)
O2−Cr2−O3	140.9(2)	O2−Cr2−O4	134.3(2)	O3−Cr2−O4	83.6(2)
O1′-Cr1′−O4′	137.4(2)	O1′-Cr1′−O3′	138.5(2)	O3′-Cr1′−O4′	82.6(2)
O2′-Cr2′−O3′	140.3(2)	O2′-Cr2′-Cr4′	135.3(2)	O3′-Cr2′−O4′	83.1(2)
Cr2−Cr1−O1	142.70(15)	Cr2−Cr1−O3	48.48(11)	Cr2−Cr1−O4	48.19(13)
Cr1−Cr2−O2	143.74(14)	Cr1−Cr2−O3	48.98(11)	Cr1−Cr2−O4	48.74(11)
Cr2′-Cr1′−O1′	144.51(16)	Cr2′-Cr1′−O3′	48.00(11)	Cr2′-Cr1′−O4′	47.50(13)
Cr1′-Cr2′−O2′	144.83(14)	Cr1′-Cr2′−O3′	48.30(11)	Cr1′-Cr2′−O4′	48.74(11)
Cr1−O3−Cr2	82.54(14)	Cr1−O4−Cr2	83.07(16)	O−Si−C$_{ave}$	107.2(8)
Cr1′−O3′-Cr2′	83.69(15)	Cr1′−O4′-Cr2′	84.66(16)	C−Si−C$_{ave}$	111.6(8)
Cr1−O1−Si1	165.0(3)	Cr1−O3−Si3	137.0(2)	Cr1−O4−Si4	139.3(3)
Cr2−O2−Si2	167.1(3)	Cr2−O3−Si3	140.2(2)	Cr2−O4−Si4	137.3(2)
Cr1′−O1′-Si1′	169.8(3)	Cr1′−O3′-Si3′	138.8(2)	Cr1′−O4′-Si4′	135.9(3)
Cr2′−O2′-Si2′	163.2(3)	Cr2′−O3′-Si3′	137.5(2)	Cr2′−O4′-Si4′	139.2(2)
Si−C−C$_{ave}$	111.9(23)	C−C−C$_{ave}$	106.8(25)		

(O$_b$)$_2$ linkages intersect at roughly 126°. As expected, the average terminal Cr−O bond distances (1.855(18) Å) are significantly shorter than the average Cr−O bond length (1.996(11) Å) ascribed to the bridging siloxides. The terminal siloxides exhibited nearly linear Cr−O−Si bond angles (166.3(28)° ave) in contrast to the substantially bent versions of the bridges (138.2(14)° ave). Each chromous center is severely distorted toward a Y-shape with the O$_b$−Cr−O$_b$ angles acute (83.0(5)° ave). The remaining O$_t$−Cr−O$_b$ angles are essentially equivalent at one chromium (Cr1, Cr1′; 137.8(6)° ave)), yet moderately disparate at the other (Cr2, 134.3(2)°, 140.9(2)°; Cr2′, 135.3(2)°, 140.3(2)°), while the coordination geometry remains roughly planar (Σ(∠OCrO) = 358.5(3)° ave). The Y-shaped conformation is reminiscent of [(^{t}Bu$_3$SiO)Cr(μ-OSi^{t}Bu$_3$)$_2$]Na·C$_6$H$_6$,[4] which possesses a (μ-O)$_2$Cr angle of 91.28(7)°, and corresponding O$_t$−Cr−(μ-O) angles of 130.95(7)° and 136.17(7)°. Its bond distances are significantly longer than those of **1**$_2$ (d(Cr−O$_t$) = 1.8906(16) Å; d(Cr−(μ-O)) = 1.9580(16) and 1.9719(14) Å), presumably because it is anionic.

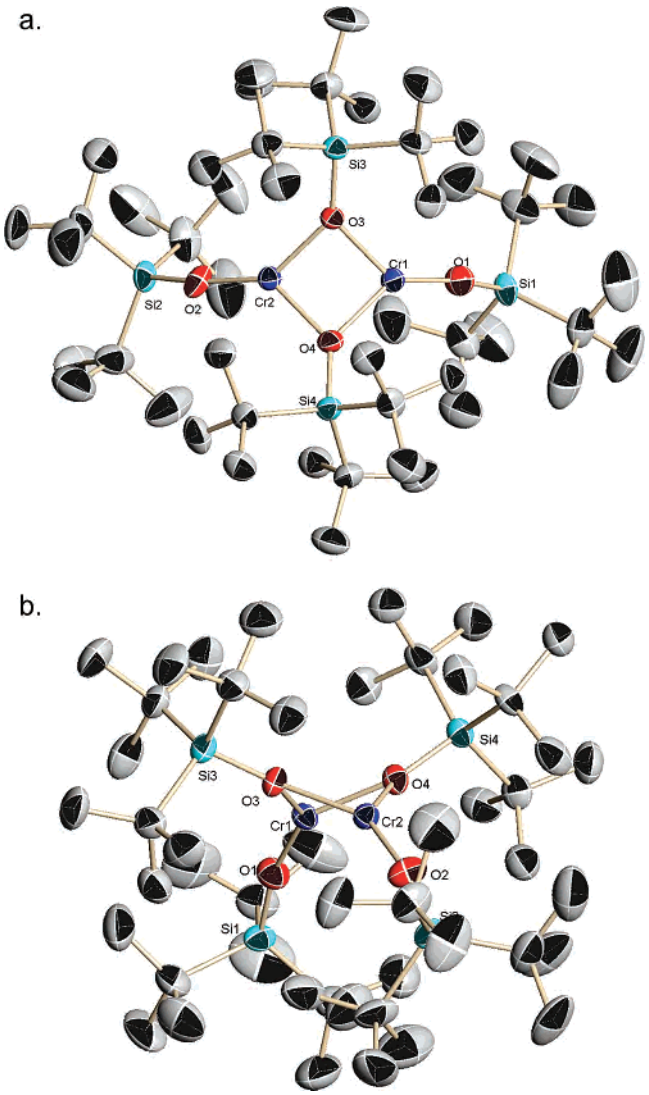

Figure 1. Molecular view (blue = Cr, red = O, teal = Si, and black = C) of [(silox)$_2$Cr] (**1**$_2$): (a) from the top; (b) from the side.

3. Magnetism. The d(Cr−Cr) in **1**$_2$ and its deviation from pseudo-D_{2h}, i.e., planar, symmetry are clearly indicative of metal−metal bonding, but to what degree is this interaction a bond, and to what extent is antiferromagnetic coupling the means by which spins pair? At room temperature, the μ_{eff} for **1**$_2$ was measured by Evans' method[16] to be 2.8 μ_B, a value suggestive of a triplet ground state and a triple bond or an antiferromagnetically coupled system.[17]

Variable-temperature magnetic susceptibility data (SQUID) revealed antiferromagnetic behavior, as illustrated by Figure 2. A relatively smooth decline in μ_{eff} vs T is evident, but there is a slight hump in the data at roughly 150 K. Lower than 100 K, there is a perceptible flattening of μ_{eff}, then a precipitous drop just before 0 K, although the system does not approach $S = 0$, remaining roughly $\mu_{eff} \approx 1.1\ \mu_B$. While the system does exhibit antiferromagnetic behavior, it is difficult to interpret the low-temperature data, especially since

(16) (a) Evans, D. F. *J. Chem. Soc.* **1959**, 2003−2005. (b) Orrell, K. G.; Sik, V. *Anal. Chem.* **1980**, *52*, 567−569. (c) Schubert, E. M. *J. Chem. Ed.* **1992**, *69*, 62.
(17) Carlin, R. L. *Magnetochemistry*; Springer-Verlag: Berlin, 1980.

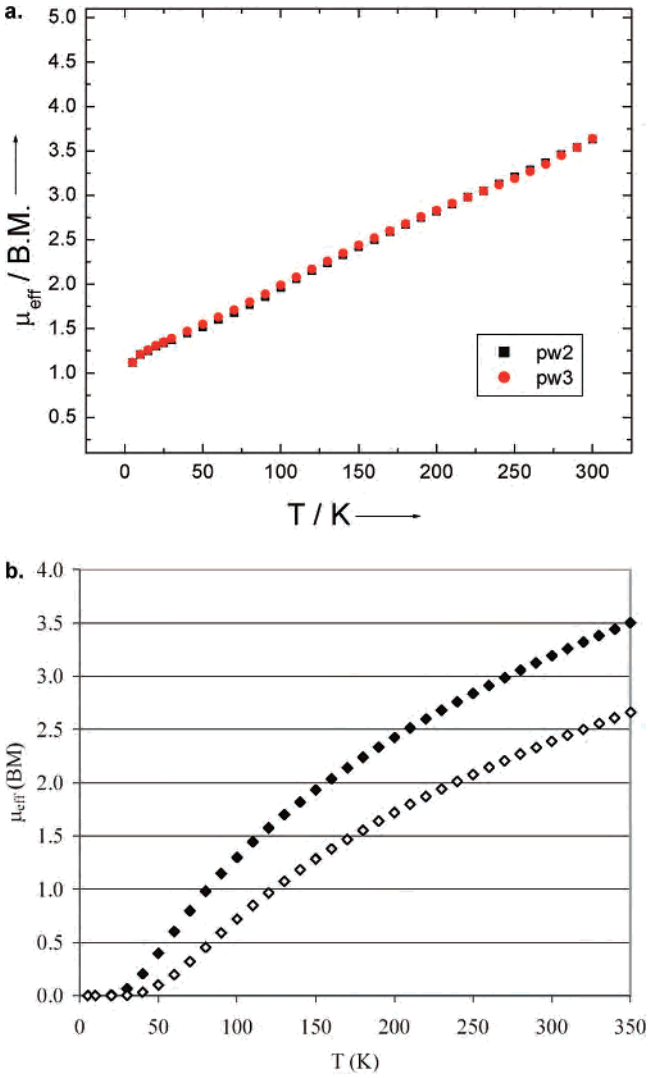

Figure 2. Magnetism of $[(^tBu_3SiO)Cr]_2(\mu\text{-}OSi^tBu_3)_2$ (**1**$_2$): (a) experimental μ_{eff} vs T plot for **1**$_2$ (two samples), and (b) calculated μ_{eff} vs T plot for $[(HO)Cr]_2(\mu\text{-}OH)_2$ (**1′**$_2$) based on a Boltzmann distribution of the $^1A_1$, $^3B_1$, $^5A_1$, $^7B_1$, and $^9A_1$ states as discussed (solid and empty diamonds represent single shell MCSCF and MRMP2 calculations, respectively).

1$_2$ is exceedingly air sensitive and small amounts of impurities can dominate the magnetism of this region. In previous runs, the >150 K data were analyzed with a dimeric Heisenberg model of $S = 2$[18] that yielded a coupling constant of $J = -200$ cm^{-1}, but fits to the low-temperature data were less than satisfactory. Noting that **1**$_2$ might have multiple open-shell states of consequence, a theoretical treatment of **1**$_2$ was utilized in assessing the T-dependence of the magnetism (vida infra).

A comparison of **1**$_2$ with other double-bridged dinuclear chromous species revealed a correlation between the room temperature μ_{eff} and the interatomic Cr···Cr separation, as Table 3 indicates.[19−22] Significant through-space spin coupling through direct d-orbital overlap between the chromous centers is likely to be the most important mechanism for antiferromagnetic coupling, hence the decline as d(Cr−Cr) increases.

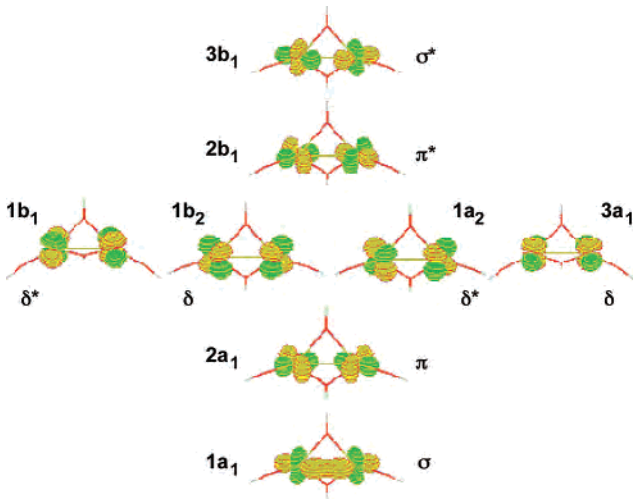

Figure 3. The eight lowest-energy MOs derived from the Cr d orbitals of $[(HO)Cr]_2(\mu\text{-}OH)_2$ (**1′**$_2$) shown are filled with eight d electrons from the two chromous ions to comprise a single shell active space.

4. Calculations. Ab initio quantum calculations were applied to $[(HO)_2Cr]_2(\mu\text{-}OH)_2$ (**1′**$_2$) using the crystallographic coordinates of one **1**$_2$ dimer (d(CrCr) = 2.68 Å) that was slightly modified to yield C_{2v} symmetry. Preliminary single-point energy calculations were applied at MCSCF/Basis Set I level of theory for all plausible spin multiplicities (1, 3, 5, 7, and 9) and active spaces symmetries (A_1, A_2, B_1, and B_2). The active space included the eight lowest-energy MOs derived from the Cr d orbitals and the eight d electrons from the two chromous ions (i.e., a single shell active space), as illustrated in Figure 3. As Table 4 indicates, the predicted low-energy states were $^1A_1$, $^3B_1$, $^5A_1$, $^7B_1$, and $^9A_1$; the next lowest state was 57 kcal/mol higher. As a consequence, only these five low-lying states were used in the subsequent calculations: MCSCF/Basis Set II and MRMP2/Basis Set I(II) for the single-shell active space, and MCSCF/Basis Set I for the double-shell active space. The double-shell active space incorporated the single-shell active space and the next eight lowest-energy MOs that subtended the same irreducible representations as the eight MOs in the single-shell active space.

The calculations showed that the method (MCSCF vs MRMP2) is more important than the basis set selection (Basis Set I vs Basis Set II) with respect to the state energy splitting. All methods indicate that the singlet gives the most stable state, and that the relative energies increase slightly with spin multiplicity. Assuming a Boltzmann distribution for the various low-energy multiplets, the calculations at the various levels of theory indicate that the ground-state electronic structure is on average 58% $^1A_1$, 31% $^3B_1$, and 9% $^5A_1$ with smaller amounts of the $^7B_1$ and $^9A_1$ states. Including the spin degeneracy, the calculated Boltzmann distribution reveals that

(18) O'Connor, C. J. *Prog. Inorg. Chem.* **1982**, *29*, 203−283.
(19) Fryzuk, M. D.; Leznoff, D. B.; Rettig, S. J.; Thompson, R. C. *Inorg. Chem.* **1994**, *33*, 5528−5534.
(20) Chisholm, M. H.; Cotton, F. A.; Extine, M. W.; Rideout, D. C. *Inorg. Chem.* **1979**, *18*, 120−125.
(21) Edema, J. J. H.; Gambarotta, S.; Meetsma, A.; Spek, A. L.; Smeets, W. J. J.; Chiang, M. Y. *J. Chem. Soc., Dalton. Trans.* **1993**, 789−797.
(22) Edema, J. J. H.; Gambarotta, S.; Spek, A. L. *Inorg. Chem.* **1989**, *28*, 812−813.

Table 3. Comparison of Interatomic d(Cr···Cr) (Å) and μ_{Eff} (μ_B at 298 K) for Various Cr(II) Dimers

compound	d(Cr···Cr)	μ_{eff}	ref
$\{[(Ph_2PCH_2SiMe_2)_2N]Cr\}_2(\mu\text{-}H)_2$	2.64	2.1	19
$[CpCr(\mu\text{-}O^tBu)]_2$	2.65	2.6	20
$[(^tBu_3SiO)Cr]_2(\mu\text{-}OSi^tBu_3)_2$ (**1**$_2$)	2.64, 2.68	2.8	this work
$[(Cy_2N)Cr]_2(\mu\text{-}NCy_2)_2$	2.84	2.6	21
$\{[(Ad)(3.5\text{-}Me_2C_6H_3)N]_2Cr\}_2(\mu\text{-}N(Ad)(3,5\text{-}Me_2C_6H_3))_2$	2.85	2.5	21
$[(^iPr_2N)Cr]_2(\mu\text{-}N^iPr_2)_2$	2.87	2.3	22
$[(thf)(Ph_2N)Cr]_2(\mu\text{-}NPh_2)_2$	3.15	3.6	21
$\{[(Ph_2PCH_2SiMe_2)_2N]Cr\}_2(\mu\text{-}Cl)_2$	3.64	6.5	19

Table 4. Calculated Relative Energies (kcal/mol) of $[(HO)Cr]_2(\mu\text{-}OH)_2$ (**1′**$_2$), a Model for $(^tBu_3SiO)Cr]_2(\mu\text{-}OSi^tBu_3)_2$ (**1**$_2$), in Different Spin States with the Calculated Magnetic Moment

	MCSCF (single shell)		MCSCF (double shell)	MRMP2 (single shell)	
electronic state	basis set I	basis set II	basis set I	basis set I	basis set II
$^1A_1$	0.00	0.00	0.00	0.00	0.00
$^3B_1$	0.29	0.29	0.35	0.44	0.44
$^5A_1$	0.87	0.85	1.07	1.32	1.32
$^7B_1$	1.73	1.68	2.13	2.68	2.63
$^9A_1$	2.84	2.76	3.56	4.58	4.48
μ_{eff} (in μ_B)	3.1	3.2	2.8	2.4	2.4

Table 5. Active Space MOs Electronic Occupation for $[(HO)Cr]_2(\mu\text{-}OH)_2$ (**1′**$_2$), a Model for $[(^tBu_3SiO)Cr]_2(\mu\text{-}OSi^tBu_3)_2$ (**1**$_2$), Calculated with MCSCF Basis Set I

	number of doubly occupied molecular orbitals				
electronic state	4	3	2	1	0
$^1A_1$	27%	9%	53%	1%	4%
$^3B_1$	–	52%	14%	23%	–
$^5A_1$	–	–	85%	4%	9%
$^7B_1$	–	–	–	100%	–
$^9A_1$	–	–	–	–	100%

the major contribution to magnetic moment is from the triplet and quintet states in a roughly 2:1 ratio: 28% for $^1A_1$, 44% for $^3B_1$, 22% for $^5A_1$, 5% for $^7B_1$, and 1% for $^9A_1$. It is reassuring to note that the double-shell MCSCF (Basis Set I) calculation reproduces the room-temperature moment (μ_{eff} = 2.8 μ_B) as observed experimentally and that all methods provided reasonable calculated values for μ_{eff} (2.4−3.2 μ_B), as Table 4 indicates.

Since the μ_{eff} vs T measurement of **1**$_2$ was conducted, the Boltzmann distribution of states was calculated as a function of temperature, and the resulting average μ_{eff} vs T plot is given in Figure 2b. The calculations manifest a roughly similar profile of antiferromagnetism from 300 to 150 K, but the $^1A_1$ state is basically the only one occupied at $T <$ 20 K. The calculations, which were done at the single-shell level for expediency, suggest that the description of the antiferromagnetic coupling in **1**$_2$ is inappropriately described by a single J and that the observed moment of ∼1.1 μ_B at 0 K may indeed be due to impurities.

The natural orbital population shows different occupations for the active space MOs, as indicated in Table 5. This variety of electron configurations is possible because the d orbitals of Cr atoms are densely packed in **1′**$_2$. Interestingly, the orbital occupancy for the $^1A_1$, $^3B_1$, and $^5A_1$ states suggests a significant antiferromagnetic arrangement of the two chromium d electrons, consistent with the observed magnetism.

$[(^tBu_3SiO)Cr]_2(\mu\text{-}OSi^tBu_3)_2$ Cleavage by L. 1. $(^tBu_3SiO)_2CrL_2$ (1-L$_2$). The Cr(II) dimer **1**$_2$ proved to be susceptible to cleavage. Treatment of **1**$_2$ with various L (L = 4-picoline,[4] *p*-tolunitrile, ^{t}BuCN, ^{t}BuNC, Ph_2CO, and PMe_3) afforded $(^tBu_3SiO)_2CrL_2$ (**1**-L$_2$) compounds, even with less than a stoichiometric amount. To cleanly form **1**-L$_2$ from **1**$_2$, typically 4 equiv of the donor were used in pentane solvent, as indicated in eq 2. Yellow crystalline *trans*-$(^tBu_3SiO)_2Cr(NCC_6H_4\text{-}p\text{-}Me)$ (**1**-(NCtol)$_2$)

$$\underset{\mathbf{1}_2}{[(^tBu_3SiO)Cr]_2(\mu\text{-}OSi^tBu_3)_2} + 4L \xrightarrow[\text{pentane}]{23\ ^\circ C} \underset{\substack{\mathbf{1}\text{-}L_2,\ L = 4\text{-pic}\ (>90\%,\ NMR),\\ NCC_6H_4\text{-}p\text{-}Me\ (93\%),\\ ^tBuCN\ (\sim 60\%),\ ^tBuNC\ (83\%),\\ Ph_2CO\ (66\%),\ PMe_3}}{2(^tBu_3SiO)_2CrL_2} \quad (2)$$

was assigned a D_{2h} structure on the basis of a single IR absorption at 2258 cm^{-1} corresponding to ν(CN) and ^{1}H NMR resonances consistent with equivalent silox and *p*-tolunitrile ligands. Its magnetic moment at room temperature was 4.8 μ_B, consistent with a chromous center. Pink *trans*-$(^tBu_3SiO)_2Cr(NC^tBu)_2$ (**1**-$(NC^tBu)_2$), which was only prepared on a small scale, showed related spectral characteristics, including a 2272 cm^{-1} band in its IR spectrum and ^{1}H NMR resonances at δ 3.04 ($\nu_{1/2} \approx$ 670 Hz) and δ 5.73 ($\nu_{1/2} \approx$ 230 Hz) that occur with a 3:1 intensity ratio.

Orange $(^tBu_3SiO)_2Cr(CN^tBu)_2$ (**1**-$(CN^tBu)_2$) exhibited one broad resonance in the ^{1}H NMR at δ 3.17 ($\nu_{1/2} \approx$ 700 Hz), but an upfield shoulder was apparent with an estimated intensity consistent with the expected 3:1 ratio. Both Nujol mull and solution IR spectra revealed a ν(CN) absorption at 2192 cm^{-1} with a minor band at 2099 cm^{-1}. Since ^{t}BuNC is a strong σ-donor and π-acceptor and possesses a correspondingly strong trans-influence, a cis-square planar geometry is conceivable, but steric influences clearly favor a trans arrangement; perhaps a mixture of these isomers is evident. Alternately, the strong σ-donating capability of ^{t}BuNC could also lead to a distortion from square planar geometry that would produce IR-active symmetric and antisymmetric stretches. Recrystallizations did not appear to change the IR; hence, minor impurities seem less likely but cannot be ruled out. The room-temperature magnetic moment of **1**-$(CN^tBu)_2$ is 4.8 μ_B, consistent with a high-spin Cr(II) center.

The intense blue color of $(^tBu_3SiO)_2Cr(PMe_3)_2$ (**1**-$(PMe_3)_2$) was distinct from the other derivatives, including the

previously prepared, lime-green *trans*-(^{t}Bu$_3$SiO)$_2$Cr(NC$_5$H$_4$-*p*-Me) (**1**-(4-pic)$_2$).[4] The ^{1}H NMR spectra showed two resonances corresponding to silox groups (δ 1.23, $\nu_{1/2} \approx 680$ Hz) and coordinated PMe$_3$ (δ 17.79, $\nu_{1/2} \approx 900$ Hz) consistent with C_2 symmetry. The deep blue color may be caused by a tetrahedral distortion from square planar geometry imposed by steric interactions between the bulky silox and PMe$_3$ groups. Unfortunately, attempts to crystallize (^{t}Bu$_3$SiO)$_2$Cr(PMe$_3$)$_2$ failed, and only blue oils were obtained.

Red-purple *trans*-(^{t}Bu$_3$SiO)$_2$Cr(OCPh$_2$)$_2$ (**1**-(OCPh$_2$)$_2$) possessed a ν(CO) at 1625 cm^{-1} with a slight shoulder at 1620 cm^{-1}, but the ^{1}H NMR spectrum was severely broadened and no discrete aryl protons could be assigned. It was possible the chromous fragment (^{t}Bu$_3$SiO)$_2$Cr (**1**) could reductively couple benzophenone to yield a pinacolate,[23] but the room-temperature magnetic moment of 4.8 μ_B supported the chromous formulation. Heating **1**-(OCPh$_2$)$_2$ in C$_6$D$_6$ at 100 °C for over a week did not result in reductive coupling chemistry. While it is conceivable that an inability to access the cis geometry necessary for benzophenone coupling is a problem, the lability of Cr(II) species, and subsequent studies, clearly suggest reductive coupling is kinetically feasible but not thermodynamically viable.

The chromous dimer **1**$_2$ and the cleavage derivatives proved to be quite air sensitive, and attempts to assay crystalline samples of **1**$_2$ and (^{t}Bu$_3$SiO)$_2$CrL$_2$ (**1**-L$_2$; L = *p*-tolunitrile, ^{t}BuNC, and Ph$_2$CO) via elemental analysis proved less than satisfactory. While ample precedent exists for square planar Cr(II) species of this type,[4,24−26] it was still disconcerting to generate elemental analyses (EAs) consistently low in carbon; hence, a structural study of **1**-(OCPh$_2$)$_2$ was obtained.

2. Structure of 1-(OCPh$_2$)$_2$. The X-ray crystal structure determination of **1**-(OCPh$_2$)$_2$ confirmed its trans square planar geometry, as shown in Figure 4. Crystal and refinement data are given in Table 1, while Table 6 lists pertinent bond distances and angles. A crystallographically imposed C_2 axis runs through the Cr atom normal to the CrO$_4$ plane, which has insignificant deviations from a true square planar geometry, as indicated by O1−Cr1−O1′ (benzophenone) and O2−Cr1−O2′ (silox) angles of 177.0(2)° and 179.8(3)°, respectively. The *d*(Cr−O(silox)) distance of 1.926(3) Å is consistent with siloxide binding to a high-spin Cr(II) center, as is the *d*(Cr−O(benzophenone)) dative bond length of 2.071(3) Å. For comparison, the chromium aryloxide distances in (2,6-^{t}Bu$_2$-4-MeC$_6$H$_2$O)$_2$Cr(THF)$_2$ are 1.948(2) Å, while its dative *d*(Cr−O(THF)) is 2.097(2) Å.[25] The silox groups bend slightly above the CrO$_4$ plane (∠Cr1−O2−Si2 = 166.9(3)°) while the benzophenones reciprocally bend below it (∠Cr1−O1−C3 = 139.8(3)°).

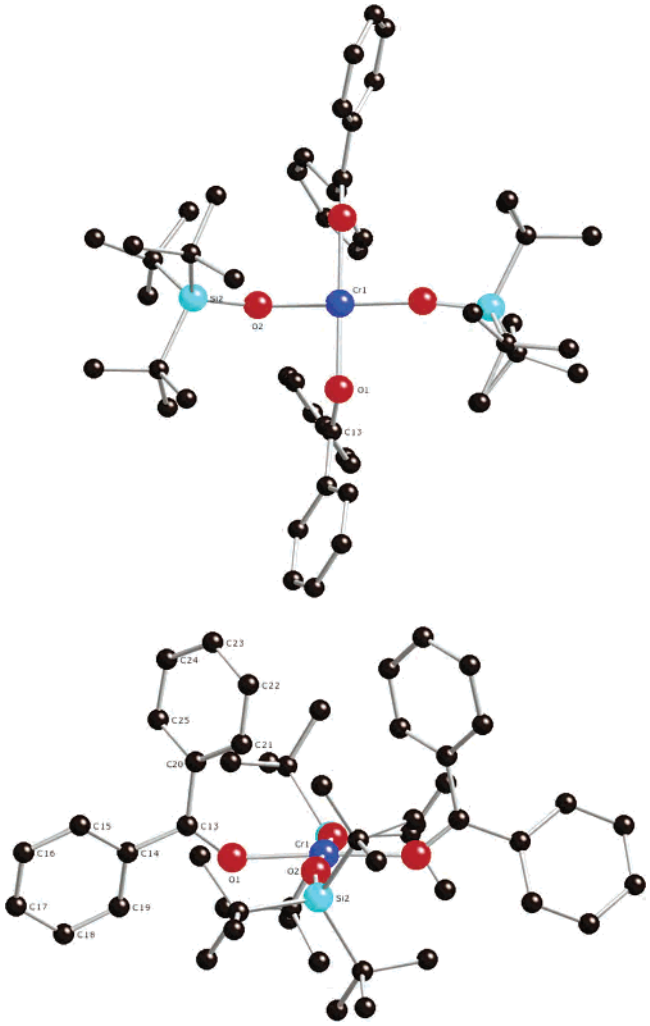

Figure 4. Molecular views of *trans*-(^{t}Bu$_3$SiO)$_2$Cr(OCPh$_2$)$_2$ (**1**-(OCPh$_2$)$_2$).

(^{t}Bu$_3$SiO)$_2$Cr(N$_2$CPh$_2$)$_2$ (2). 1. Synthesis. Given the observed cleavage chemistry, **1**$_2$ appeared to be a ready source of Cr(II). With the possibility of generating a Cr(IV) alkylidene in mind, **1**$_2$ was treated with diphenyldiazomethane in pentane,[27−29] resulting in the immediate formation of a dark brown solution from which crystals of (^{t}Bu$_3$SiO)$_2$Cr(N$_2$CPh$_2$)$_2$ (**2**) were isolated in 50% yield according to eq 3. The ^{1}H and ^{13}C{^{1}H} NMR spectra of diamagnetic **2** revealed one

$$\underset{\mathbf{1}_2}{[(^t\mathrm{Bu_3SiO})\mathrm{Cr}]_2(\mu\text{-}\mathrm{OSi}^t\mathrm{Bu_3})_2} + 4\mathrm{N_2CPh_2} \xrightarrow[\text{pentane}]{23\ ^\circ\mathrm{C}} \underset{\mathbf{2}}{2(^t\mathrm{Bu_3SiO})_2\mathrm{Cr}(=\mathrm{N}-\mathrm{N}=\mathrm{CPh_2})_2} \quad (3)$$

type of silox ligand and one set of aryl resonances consistent with a C_{2v} bis-diphenylmethylidenehydrazido complex. This unusual 4e$^-$ oxidation to Cr(VI) prompted verification of the structure by X-ray methods. While **2** is stable for weeks at −30 °C, it degrades rapidly at 23 °C in benzene-d_6 ($t_{1/2} \approx$

(23) McMurry, J. E. *Chem. Rev.* **1989**, *89*, 1513−1524.
(24) Terry, K. W.; Gantzel, P. K.; Tilley, T. D. *Inorg. Chem.* **1993**, *32*, 5402−5404.
(25) Edema, J. J. H.; Gambarotta, S. van Bolhuis, F.; Smeets, W. J. J.; Spek, A. L. *Inorg. Chem.* **1989**, *28*, 1407−1410.
(26) Edema, J. J. H.; Gambarotta, S.; van Bolhuis, F. Spek, A. L. *J. Am. Chem. Soc.* **1989**, *111*, 2142−2147.
(27) Herrmann, W. A. *Angew. Chem., Int. Ed. Engl.* **1978**, *17*, 800−812.
(28) Trnka, T. M.; Grubbs, R. H. *Acc. Chem. Res.* **2001**, *34*, 18−29.
(29) Dartiguenave, M.; Menu, M. J.; Deydier, E.; Dartiguenave, Y.; Siebald, H. *Coord. Chem. Rev.* **1998**, *178−180*, 623−663.

Table 6. Selected Interatomic Distances (Å) and Angles (deg) in *trans*-(^{t}Bu$_3$SiO)$_2$Cr(OCPh$_2$)$_2$ (**1**-(OCPh$_2$)$_2$)

Cr1−O1	2.071(3)	Cr1−O2	1.926(3)	Si2−O2	1.596(3)
O1−C3	1.245(6)	C3−C4	1.479	C3−C9	1.481(6)
Si−C$_{ave}$	1.934(6)	C−C(silox)$_{ave}$	1.52(2)	C−C(Ph)$_{ave}$	1.388(15)
O1−Cr1−O2	87.31(12)	O1−Cr1−O1′	177.0(2)	O1−Cr1−O2′	92.68(12)
O2−Cr−O2′	179.8(3)	Cr1−O2−Si2	166.9(3)	Cr1−O1−C3	139.8(3)
O1−C3−C4	119.3(4)	O1−C3−C9	199.9(4)	C3−C−C$_{ave}$	120.2(6)
O−Si−C$_{ave}$	108.5(10)	C−Si−C$_{ave}$	110.4(6)	Si−C−C$_{ave}$	112.2(32)
C−C−C(silox)$_{ave}$	106.5(19)	C−C−C(Ph)$_{ave}$	120.0(6)		

Table 7. Selected Interatomic Distances (Å) and Angles (deg) in (^{t}Bu$_3$SiO)$_2$Cr(N$_2$CPh$_2$)$_2$ (**2**)

Cr1−O1	1.803(2)	Cr1−O2	1.802(2)	Cr1−N1	1.664(3)
Cr1−N3	1.666(2)	Si1−O1	1.644(2)	Si2−O2	1.644(2)
N1−N2	1.319(4)	N3−N4	1.301(4)	N2−C25	1.317(4)
N4−C38	1.321(4)	C25−C26	1.475(5)	C25−C32	1.470(5)
C38−C39	1.481(5)	C38−C45	1.466(5)	Si−C$_{ave}$	1.928(5)
C−C(silox)$_{ave}$	1.539(9)	C−C(Ph)$_{ave}$	1.385(13)		
O1−Cr1−O2	118.46(11)	O1−Cr1−N1	110.48(12)	O1−Cr1−N3	107.02(12)
O2−Cr−N1	105.86(12)	O2−Cr1−N3	108.78(11)	N1−Cr1−N3	105.54(14)
Cr1−O1−Si1	148.66(15)	Cr1−O2−Si2	149.27(15)	Cr1−N1−N2	150.2(2)
Cr1−N3−N4	150.4(3)	N1−N2−C25	119.5(3)	N3−N4−C38	119.6(3)
N2−C25−C26	124.3(3)	N2−C25−C32	116.3(3)	N4−C38−C39	122.5(3)
N4−C38−C45	116.7(3)	C26−C25−C32	119.4(3)	C39−C38−C45	120.9(3)
C25−C26−C27	119.1(3)	C25−C26−C31	122.8(3)	C25−C32−C33	121.6(3)
C25−C32−C37	119.3(3)	C38−C39−C40	119.8(3)	C38−C39−C44	122.0(3)
C38−C45−C46	120.4(4)	C38−C45−C50	121.3(4)	O−Si−C$_{ave}$	106.5(25)
C−Si−C$_{ave}$	112.3(3)	Si−C−C$_{ave}$	111.5(16)	C−C−C(silox)$_{ave}$	107.3(10)
C−C−C(Ph)$_{ave}$	120.1(9)				

Table 8. Selected Interatomic Distances (Å) and Angles (deg) in (^{t}Bu$_3$SiO)$_2$Cr═N(2,6-Ph$_2$-C$_6$H$_3$) (**3**-(2,6-Ph$_2$-C$_6$H$_3$))

Cr1−O1	1.7800(19)	Cr1−O2	1.7802(18)	Cr1−N1	1.649(2)
Si1−O1	1.630(2)	Si2−O2	1.6332(19)	N1−C12	1.372(3)
C6−C7	1.486(4)	C11−C13	1.490(4)	C−C(Ph)$_{ave}$	1.385(17)
Si−C$_{ave}$	1.921(6)	C−C(silox)$_{ave}$	1.54(8)[a]		
O1−Cr1−O2	122.02(10)	O1−Cr1−N1	118.93(11)	O2−Cr1−N1	118.96(10)
Cr1−O1−Si1	155.77(19)	Cr1−O2−Si2	154.64(13)	Cr1−N1−C12	175.9(2)
N1−C12−C7	119.8(2)	N1−C12−C11	119.0(2)	C−C−C(Ph)$_{ave}$	120.3(11)
O−Si−C$_{ave}$	106.2(15)	C−Si−C$_{ave}$	112.5(6)	Si−C−C$_{ave}$	111.4(41)[a]
C−C−C(silox)$_{ave}$	107.8(21)	C−C−C(Ph)$_{ave}$	120.1(9)		

[a] Error reflects disorder in two *tert*-butyl groups.

6 h) and in the solid state ($t_{1/2} \approx 1$ week); it degrades completely within minutes at 80 °C in C_6D_6. ^{1}H NMR spectra of the degradation product(s) were indicative of two species, one paramagnetic and one diamagnetic, but no further characterization was attempted.

2. Molecular Structure. Data and refinement information pertaining to **2** are given in Table 1, while pertinent bond distances and angles are listed in Table 7. As Figure 5 illustrates, **2** is pseudo-tetrahedral, as expected for a four-coordinate Cr(VI) complex, with a slightly splayed O1−Cr1−O2 angle of 118.46(11)° in comparison to the 105.54-(14)° angle subtended by the diphenylmethylidenehydrazido nitrogens. The remaining O−Cr−N angles are between these values: ∠O1−Cr−N1,N3 = 110.48(12)°, 107.02(12)° and ∠O2−Cr−N1,N3 = 105.86(12)°, 108.78(11)°. The Cr(VI)−oxygen siloxide distances of 1.803(2) and 1.802(2) Å are significantly shorter than the aforementioned bonds to Cr(II), as expected.[30] The Cr−O−Si angles are more bent than usual (148.66(15)°, 149.27(15)°), perhaps reflecting the steric influence of the diphenylmethylidenehydrazido linkages. The Cr(VI)−N bond lengths of 1.664(2) and 1.666(2) Å are normal for dianionic nitrogen-based ligands,[31] and the N−N bond distances of 1.319(4) and 1.301(4) Å fall between those of PhN═NPh (1.26 Å)[32] and PhHC═N−N═CHPh (1.32 Å),[33] while clearly remaining sp^2-hybridized at the β-nitrogens, as the N−N−C bond angles (119.5(3)°, 119.6(3)°) indicate. Coupled with the Cr−N−N bond angles of 150.2-(2)° and 150.4(3)°, the data suggest contributions from CrN double- (A) and triple-bonded (B) resonance structures, as indicated by Figure 6.[29,34] The slightly short N−N distances may reflect α-nitrogens whose hybridization is between sp and sp^2 due to the chromium−nitrogen multiple bonding or some charge distribution into the phenyl groups (C), as the subtly long N−C bond distances (1.317(4), 1.321(4) Å) imply (normal bond lengths: C═N, 1.28 Å; C−N(sp^2), 1.38 Å).

[(^{t}Bu$_3$SiO)Cr]$_2$(μ-OSi^{t}Bu$_3$)$_2$ Cleavage by RN$_3$. 1. Synthesis of (^{t}Bu$_3$SiO)$_2$Cr(═NR)$_x$ (x = 1, 3-R; 2, 4-R). While the addition of diphenyldiazomethane to **1**$_2$ failed to yield an alkylidene via N_2 loss,[27−29] organoazide additions[35]

(30) Coles, M. P.; Gibson, V. C.; Clegg, W.; Elsegood, M. R. J. *Polyhedron* **1998**, *17*, 2483−2489.

(31) Nugent, W. A.; Mayer, J. M. *Metal−Ligand Multiple Bonds*; Wiley-Interscience: New York, 1988.

(32) Brown, C. J. *Acta Crystallogr.* **1966**, *21*, 146−152.

(33) Sinha, U. C. *Acta Crystallogr.* **1970**, *B26*, 889−895.

(34) Mizobe, Y.; Ishii, Y.; Hidai, M. *Coord. Chem. Rev.* **1995**, *139*, 281−311.

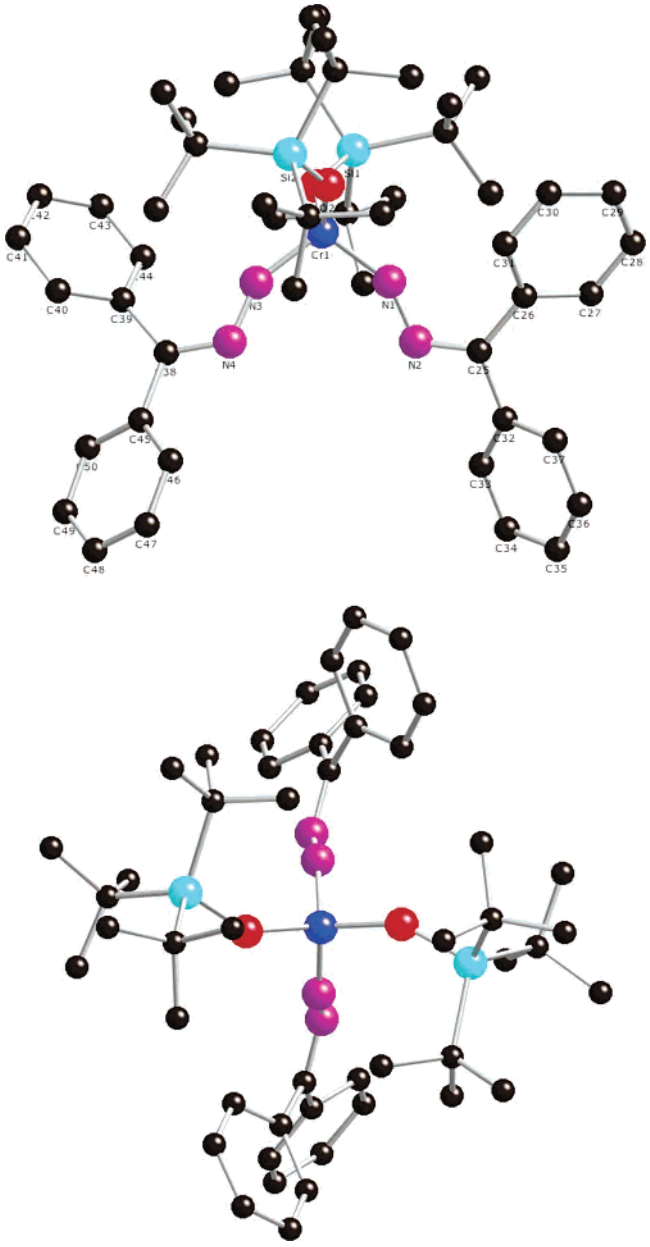

Figure 5. Molecular views of $(^tBu_3SiO)_2Cr(N_2CPh_2)_2$ (**2**).

resulted in dimer cleavage and formation of unusual Cr(IV) mono-imido species or the Cr(VI) diimido complexes according to eqs 4 and 5. For bulky RN_3 (R = adamantyl (Ad), 2,6-^{i}Pr$_2$-C$_6$H$_3$, 2,4,6-Me$_3$-C$_6$H$_2$ = Mes, 2,6-Ph$_2$-C$_6$H$_3$), the paramagnetic, Cr(IV)

$$\underset{\mathbf{1}_2}{[(^tBu_3SiO)Cr]_2(\mu\text{-}OSi^tBu_3)_2} + 2N_3R \xrightarrow[\text{pentane}]{23\ ^\circ C} \underset{\substack{\mathbf{3}\text{-R (R = Ad, 2,6-}^i\text{Pr}_2\text{-C}_6\text{H}_3,\\ \text{2,4,6-Me}_3\text{-C}_6\text{H}_2\text{, 2,6-Ph}_2\text{-C}_6\text{H}_3)}}{2(^tBu_3SiO)_2Cr{=}NR} + 2N_2 \quad (4)$$

$$\underset{\mathbf{1}_2}{[(^tBu_3SiO)Cr]_2(\mu\text{-}OSi^tBu_3)_2} + 4N_3R \xrightarrow[\text{benzene}]{23\ ^\circ C} \underset{\mathbf{4}\text{-R (R = 1-Naph, 2-Anth)}}{2(^tBu_3SiO)_2Cr(=NR)_2} + 4N_2 \quad (5)$$

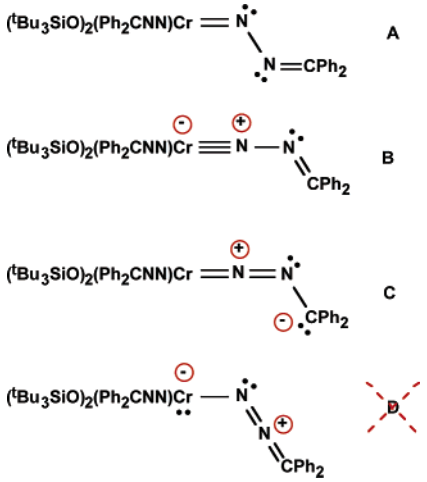

Figure 6. Resonance contributions relevant to the hydrazido bonding in $(^tBu_3SiO)_2Cr(N_2CPh_2)_2$ (**2**). Structures A, B, and C are significant, while D is not likely.

monoimido (silox)$_2$Cr=NR (**3**-R) was the major product. Difficulties in obtaining X-ray-quality crystals of **3**-R prompted the use of 1-azidonaphthalene and 2-azidoanthracene, but these smaller substrates afforded the diamagnetic Cr(VI) diimido species $(^tBu_3SiO)_2Cr(=NR)_2$ (**4**-R, R = 1-Naph, 2-Anth) along with unreacted $\mathbf{1}_2$, implicating the stoichiometry given in eq 5. It appears that azide oxidation of Cr(IV) to Cr(VI) is swifter than the initial Cr(II)-to-Cr(IV) imide formation, unless the second reaction is sterically

$$\underset{\mathbf{3}\text{-Ad}}{(^tBu_3SiO)_2Cr{=}NAd} + AdN_3 \xrightarrow[\text{benzene-}d_6]{100\ ^\circ C,\ 4\ h} \underset{\mathbf{4}\text{-Ad}}{(^tBu_3SiO)_2Cr(=NAd)_2} + N_2 \quad (6)$$

impeded. Treatment of **3**-Ad with another equiv of AdN_3 yielded **4**-Ad, but only after heating at 100 °C for several hours (eq 6); **4**-Ad was also prepared via eq 5. NMR spectra of **4**-Ad correlated nicely with that previously reported for $(Me_3SiO)_2Cr(=NAd)_2$.[30]

2. Molecular Structure of $(^tBu_3SiO)_2Cr{=}N(2,6\text{-}Ph_2\text{-}C_6H_3)$ (3-(2,6-Ph$_2$-C$_6$H$_3$)). Data and refinement information for $(^tBu_3SiO)_2Cr{=}N(2,6\text{-}Ph_2\text{-}C_6H_3)$ (**3**-(2,6-Ph$_2$-C$_6$H$_3$)) have been tabulated (Table 1), its bond distances and angles are listed in Table 7, and a molecular view is shown in Figure 7. The molecule crystallizes in a chiral space group due to the cant of the ortho phenyl substituents on the terphenyl

(35) For a selection imido syntheses from RN_3, see: (a) Schweda, E.; Scherfise, K. D.; Dehnicke, K. *Z. Anorg. Allg. Chem.* **1985**, *528*, 117−124. (b) Cummins, C. C.; Schrock, R. R.; Davis, W. M. *Inorg. Chem.* **1994**, *33*, 1448−1457. (c) Fickes, M. G.; Davis, W. M.; Cummins, C. C. *J. Am. Chem. Soc.* **1995**, *117*, 7, 6384−6385. (d) Elliott, R. L.; Nichols, P. J.; West, B. O. *Polyhedron* **1987**, *6*, 2191−2192. (e) Chou, C. Y.; Huffman, J. C.; Maatta, E. A. *J. Chem. Soc., Chem. Commun.* **1984**, *17*, 1184−1185. (f) Maatta, E. A.; Du, Y.; Rheingold, A. L., *J. Chem. Soc., Chem. Commun.* **1990**, *10*, 756−757. (g) Lichtenhan, J. D.; Critchlow, S. C.; Doherty, N. M., *Inorg. Chem.* **1990**, *29*, 439−442. (h) Chisholm, M. H.; Folting, K.; Huffman, J. C.; Kirkpatrick, C. C.; Ratermann, A. L. *J. Am. Chem. Soc.* **1981**, *103*, 1305−1306. (i) Listemann, M. L.; Schrock, R. R.; Dewan, J. C.; Kolodziej, R. M. *Inorg. Chem.* **1988**, *27*, 264−271. (j) Hillhouse, G. L.; Haymore, B. L. *J. Organomet. Chem.* **1978**, *162*, C23−C26. (k) Danopoulos, A. A.; Redshaw, C.; Vaniche, A.; Wilkinson, G.; Hussain-Bates, B.; Hursthouse, M. B. *Polyhedron* **1993**, *12*, 1061−1071.

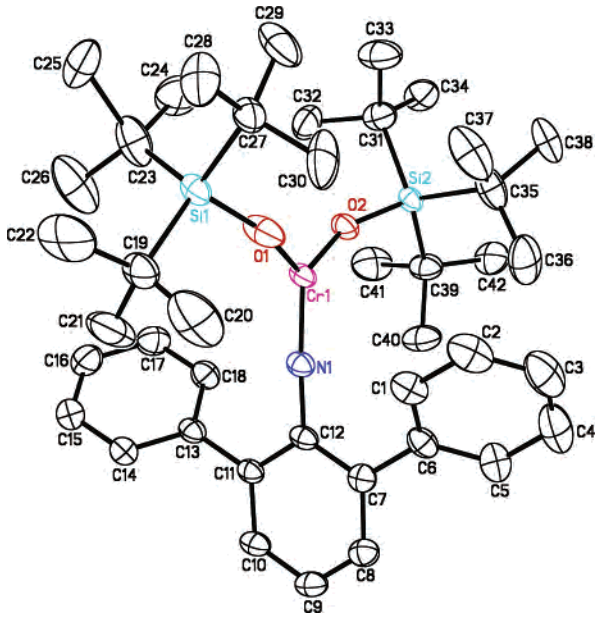

Figure 7. Molecular view of $(^tBu_3SiO)_2Cr{=}N(2,6\text{-}Ph_2\text{-}C_6H_3)$ (**3**-(2,6-Ph_2-C_6H_3)).

fragment that impart a C_2 symmetry to **3**-(2,6-Ph_2-C_6H_3). The complex is virtually trigonal in terms of its core angles, with ∠O1−Cr1−O2 = 122.02(10)°, ∠O1−Cr1−N1 = 118.93(11)° and ∠O2−Cr1−N1 = 118.96(10)°. The chromium−nitrogen distance of 1.649(2) Å is normal, as are the *d*(CrO) of 1.7800(19) and 1.7802(18) Å, and the accompanying Cr1−N1−C12 angle of 175.9(2)° suggests that a triple bond is present, albeit one with disparate π bonds due to interactions with energetically different d_{xz} and d_{yz} orbitals.

3. Calculations on $(H_3SiO)_2Cr{=}NPh$ (3″-Ph). In reference to **3**-(2,6-Ph_2-C_6H_3), density functional calculations on $(H_3SiO)_2Cr{=}NPh$ (**3″**-Ph) were conducted. Figure 8 illustrates the geometries of the ground state (GS) triplet (T) and lowest excited state (ES) singlet (S) species. For the GS triplet (a), the bond distances are all within 0.03 Å of those observed for **3**-(2,6-Ph_2-C_6H_3), and all the angles are within a few degrees, but the phenyl group is in the trigonal plane rather than perpendicular to it. The silox groups are an obvious steric influence on the phenyl group geometry in **3**-(2,6-Ph_2-C_6H_3); thus, the phenyl group in **3″**-Ph was artificially rotated to see whether the orbital energies in Figure 9 are germane to the real system. Little change was noted; hence, the calculated **3″**-Ph geometry and orbital energies were deemed sufficiently accurate to discuss. Two ES singlet minima corresponding to in-plane and perpendicular phenylimido structures were found. The in-plane geometry was lower in energy, leading to a +14.3 kcal/mol S/T energy gap, but the perpendicular geometry (S/T gap = 15.0 kcal/mol) was considered more relevant given the aforementioned steric influences, and the orbitals in Figure 9 correspond to this model. Note that the singlet ES conformation manifests changes from the GS that include significantly shortened Cr−O (by 0.04 Å) and Cr−N (by 0.02 Å) distances, a more open O−Cr−O angle of 127.7° and correspondingly lesser O−Cr−N angles of 115.4° and 116.5°.

The d-orbital splitting diagrams and corresponding orbital energies for the GS and ES species are given in Figure 9. In the GS, the lowest orbital is d_{z^2}, which is basically nonbonding, and it contains one electron. One might expect d_{z^2} to have some σ* character, but in this low-symmetry environment, a higher-energy "4s orbital" contains this component. The next orbital is d_{yz}, which is π antibonding with respect to an antisymmetric combination of siloxide oxygen p_z orbitals, and it is 0.45 eV above d_{z^2} and contains one electron. There is a rather large energy gap (1.14 eV) before the next, unoccupied orbital, which is d_{xz}, an orbital that is π* with respect to the imido nitrogen and π* with respect to a symmetric combination of silox oxygen p_z orbitals. Next comes $d_{x^2-y^2}$, which has predominantly CrN σ* character, but is also π* with respect to the in-plane symmetric combination of silox oxygen p_x orbitals. It resides 0.59 eV above d_{xz} but 0.69 eV below the highest orbital, d_{xy}, which is basically CrO σ* in character and π* with respect to the in-plane CrN π interaction.

At ∼15 kcal/mol above the GS, the ES singlet cannot be thermally poplulated to any significant extent. A pair of electrons resides in d_{z^2}, and the remaining orbital ordering and composition is similar to the GS except for a switch in $d_{x^2-y^2}$ and d_{xy}. The huge energy gap between d_{z^2} and d_{yz} (3.87 eV!) is in part due to increase in the O−Cr−O angle from ∼119° to 128°, which imparts far greater π* character with respect to the antisymmetric combination of oxygen p_z orbitals. This same distortion places greater Cr−O σ* character to $d_{x^2-y^2}$, causing it to increase in energy and rise above d_{xy} whose oxygen σ* character is partly diminished. The *total* energetics of the GS and ES must be assessed to understand the nature of the S/T gap of 15 kcal/mol. Figure 9 focuses on the frontier orbital energetics, but it is the energies of the ligand-localized orbitals (not shown) that dominate the total energies of the triplet GS and single ES.

Discussion

Chromous Dimer, 1_2. The butterfly arrangement of 1_2, while structurally related to some of the μ-amido species in Table 3, is different than Powers' dialkoxide, $[(^tBu_3CO)Cr]_2(\mu\text{-}OCH^tBu_2)_2$,[36] which possesses a planar core. Unfortunately, electronic features of the chromous alkoxide, which is generated via thermal degradation of $(^tBu_3CO)Cr(\mu\text{-}Cl)(\mu\text{-}OC^tBu_3)Li(THF)_2$,[37] were not investigated. Curiously, in the crystal structure of $[(^tBu_3CO)Cr]_2(\mu\text{-}OCH^tBu_2)_2$, there are two independent molecules with *d*(Cr···Cr) of 3.075(1) and 3.042(1) Å, whose difference is quite similar to that of the crystallographically independent molecules of 1_2. The modest geometric changes between the siloxide and alkoxide dinuclear complexes, which may be steric in nature, perhaps testify to the weak metal−metal interactions intrinsic in these chromous systems.

While it is tempting to describe the antiferromagnetic interaction in 1_2 and like compounds with a single *J*—and

(36) Murray, B. D.; Hope, H.; Power, P. P. *J. Am. Chem. Soc.* **1985**, *107*, 169−173.
(37) Hvoslef, J.; Hope, H.; Murray, B. D.; Power, P. P. *Chem. Commun.* **1983**, 1438−1439.

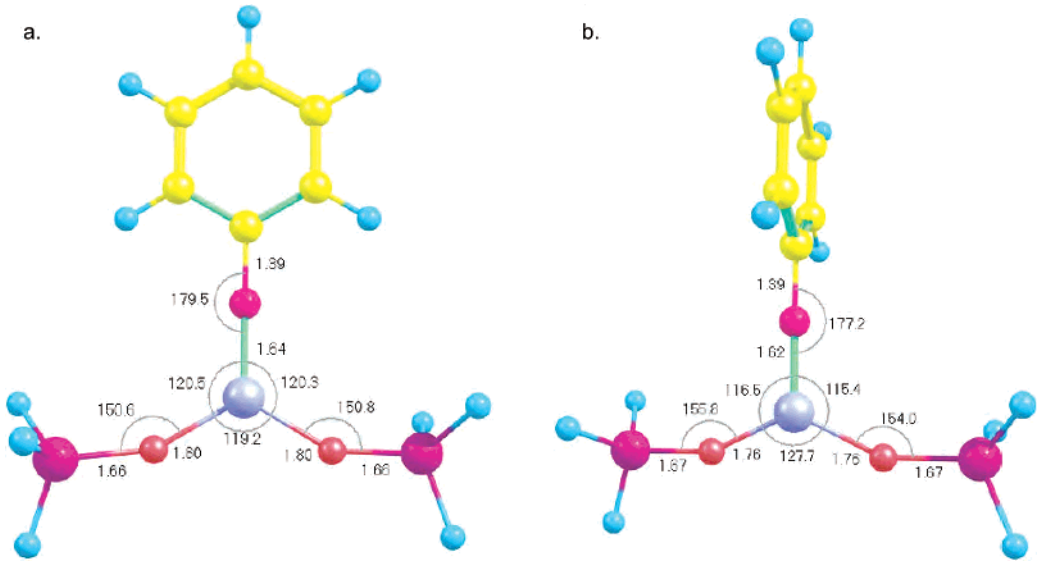

Figure 8. $(H_3SiO)_2Cr{=}NPh$ (**3″**-Ph) geometries pertaining to the ground-state triplet (a) and first excited-state singlet (b) states.

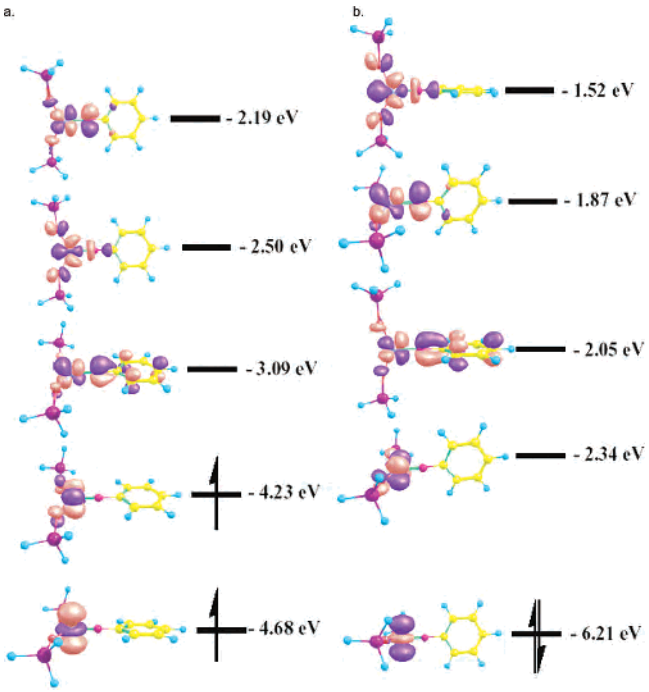

Figure 9. $(H_3SiO)_2Cr{=}NPh$ (**3″**-Ph, *z* perpendicular to the trigonal plane, *x* along the CrN vector) selected orbital energies pertaining to the ground-state triplet (a) and first excited-state singlet (b) states.

for comparison sake this still may be useful—the calculations show that the magnetic properties of dichromous systems may require inclusion of a greater number of states. In this instance, while the major contributors were the $^3B_1$ and $^5A_1$ states, inclusion of minor $^1A_1$, $^7B_1$ and even 1% of the $^9A_1$ proved to aid in the estimation of the magnetism. There is still a discrepancy between the low-temperature μ_{eff} vs T observed and calculated plots (Figure 2), but the air sensitivity of $\mathbf{1}_2$ and the plausible contribution of paramagnetic impurities (probably Cr(III)) at $T < 50$ K render a discussion of the differences somewhat specious. In view of the magnetism and calculations, as well as the ready cleavage of $\mathbf{1}_2$, the dichromium interaction is best considered one of strong antiferromagnetic character.

$\mathbf{1}_2$ as a Source of "(silox)$_2$Cr" (1). A variety of donors (L) severed the $Cr_2(\mu\text{-}OSi^tBu_3)_2$ core of $\mathbf{1}_2$ to produce $(silox)_2CrL_2$ (**1**-L_2, L = 4-picoline, *p*-tolunitrile, ^{t}BuCN, ^{t}BuNC, Ph_2CO, and PMe_3)). Four-coordinate high-spin Cr(II) complexes have a preference for square planar geometry, as seen previously in the cleavage of $[Cr(\mu\text{-}OSi^tBu_3)(\mu\text{-}Cl)]_4$ by THF and 4-picoline to afford *trans*-$(^tBu_3SiO)ClCr(THF)_2$ and *trans*-$(^tBu_3SiO)_2Cr(NC_5H_4\text{-}p\text{-}Me)_2$ (**1**-$(4\text{-pic})_2$).[4] Other alkoxide and siloxide species such as $Cr\{OSi(O^tBu)_3\}_2(NHEt_2)_2$,[24] *trans*-$Cr(OR)_2(THF)_2$[25] (R = 2,6-di-^{t}Bu-4-methylphenyl), and $[(TMEDA)Na]_2Cr(OR')_4$[26] are also known. The only unusual cleavage product is **1**-$(PMe_3)_2$, whose intense blue color contrasts with the more muted hues of the known square planar derivatives. The possibility exists that square planar ⇄ tetrahedral isomerizations akin to the classic d^8 $L_2Ni^{II}X_2$ cases[38] may be operational for this chromous system. It is here that the bulk of the silox ligand might enable the observation of pseudo-T_d complexes via relief of steric congestion with large L such as PMe_3.

Adduct (i.e., $(silox)_2CrL_2$ (**1**-L_2)) formation, the generation of **2** from $\mathbf{1}_2$ and Ph_2CNN, and **3**-R synthesis from $\mathbf{1}_2$ and RN_3 essentially occur upon mixing of the reagents. It is tempting to conclude that L or Ph_2CNN or RN_3 must be reacting directly with the $Cr_2(\mu\text{-}OSi^tBu_3)_2$ core, but a rapid equilibrium between dimer and monomer, i.e., $\mathbf{1}_2 \rightleftarrows 2(^tBu_3SiO)_2Cr$ (**1**), cannot be ruled out. Assuming **1** would be rapidly trapped by L, and estimating a "mixing time", τ, of 1 s (roughly the reaction time as observed by the color change), then the dissociation of $\mathbf{1}_2$ would be roughly 1 s^{-1} ($\Delta G^{\ddagger} \approx 17$ kcal/mol), which is certainly with reason for a weakly metal−metal-bonded dinuclear complex. Given the rates, regardless of mechanism, it is certainly reasonable to consider $\mathbf{1}_2$ as a source of "$(silox)_2Cr$ (**1**)".

Dihydrazide 2. While the bis-diphenylmethylidenehydrazido species **2** is unusual, it is not unique. One of the earliest diazoalkane complexes with similar M−NNC bond-

(38) Pinolet, L. H.; Horrocks, W. DeW. Jr.; Holm, R. H. *J. Am. Chem. Soc.* **1970**, *92*, 1855−1863 and references therein.

ing parameters to **2** was observed by Chisholm and co-workers.[39] The dinuclear complex, [(^{i}PrO)$_2$(Ph$_2$CN$_2$)Mo](μ-O^{i}Pr)$_3$[Mo(N$_2$CPh$_2$)(O^{i}Pr)(py)], has a single Mo−Mo bond, and both diphenylmethylidenehydrazido ligands are terminal. First-row transition row transition metal complexes derived from diazoalkane complexes are less common, but several have been structurally characterized including Cp$_2$Ti(N$_2$-CPh$_2$)(PMe$_3$),[40] [(Me$_3$Si)$_2$N]$_2$V(N$_2$CPh$_2$)(Cl),[41] and (ArN═)$_2$-Cr(N$_2$CPh$_2$)(PMe$_3$).[42] What is unique about the conversion of **1**$_2$ to **2** upon addition of Ph$_2$CNN is the conversion of Cr(II) to Cr(VI), but this is mostly a consequence of the lack of chromous reagents that could accommodate two of the diphenylmethylidenehydrazido ligands.

Imido Derivatives (^{t}Bu$_3$SiO)$_2$Cr(═NR)$_x$ (x = 1, 3-R; 2, 4-R). A brief look at the literature reveals that the bis-imido species **4**-R are rather common, but the mono-imido **3**-R complexes are rare. Numerous Cr(VI) imido complexes have been characterized in the literature beginning with Nugent and co-workers, who isolated (Me$_3$SiO)$_2$Cr(═N^{t}Bu)$_2$ from the treatment of CrO$_2$Cl$_2$ with ^{t}Bu(SiMe$_3$)NH.[43] Subsequent cleavage of the siloxide linkage with BCl$_3$ yielded Cl$_2$Cr(═N^{t}Bu)$_2$,[44] and both species act as precursors to a variety of other Cr(VI) organoimido species.[45−47] Well-characterized monomeric reduced chromium imido species are less prevalent than their Cr(VI) analogues.[48] Cr(V) imido species tend to dimerize via imido bridges to maintain tetrahedral coordination in the absence of bulky ligands or a coordinating solvent. Oxidation of [CpCrCl$_2$]$_2$ with Me$_3$SiN═NSiMe$_3$ yielded the Cr(V) dimer [CpCr═NSiMe$_3$]$_2$(μ-NSiMe$_3$)$_2$,[49] while reduction of Cl$_2$Cr(═N^{t}Bu)$_2$ with cobaltocene gave the related [ClCr═N^{t}Bu]$_2$(μ-N^{t}Bu)$_2$.[50] The monomeric Cr(V) species ^{t}BuN═CrCl$_3$L$_2$ (L = PEt$_2$Ph, THF, py, 0.5DME) were obtained from the reductive chlorination of Cl$_2$Cr(═N^{t}Bu)$_2$ to form [^{t}BuN═CrCl$_3$]$_x$, which was then treated with L[48] and often derivatized further.[46]

The structure of **3**-(2,6-Ph$_2$-C$_6$H$_3$) is related to the previously characterized W(IV) monomer, (^{t}Bu$_3$SiO)$_2$W═N^{t}Bu.[51] Both are planar and pseudo-trigonal, but the tungsten derivative is low spin, while **3**-(2,6-Ph$_2$-C$_6$H$_3$) and the other **3**-R RN$_3$ (R = Ad, 2,6-^{i}Pr$_2$-C$_6$H$_3$, Mes) appear to possess S = 1 ground states according to their nearly spin-only μ_{eff} values at room temperature. As the d-orbital splitting diagram in Figure 9 reveals, the d_{z^2} is proximate to d_{yz} in energy for the Cr complex, whereas in W, the d_{z^2} orbital is likely to be energetically quite lower. It is this stability of d_{z^2} which appears to be a critical factor in rendering third-row d^2 species diamagnetic (e.g., Ta,^{2} W).[52]

One example of a structurally characterized,[46] monomeric Cr(IV) organoimido complex is *trans*-[CrCl(NEt)(dmpe)$_2$]-[SO$_3$CF$_3$], which was prepared by Wilkinson et al. upon addition of addition of Ba(O$_3$SCF$_3$)$_2$ to a methanol solution of *trans*-[CrCl(NCMe)(dmpe)$_2$][BPh$_4$].[53] Magnesium reduction of (ArN)$_2$CrCl$_2$ (Ar = 2,6-^{i}Pr$_2$C$_6$H$_3$) in the presence of 2 equiv of PR$_3$ (R═PMe$_3$,PMe$_2$Ph) yielded diamagnetic (ArN)$_2$Cr(PR$_3$)$_2$,[42] while West and co-workers[54] synthesized the high-spin Cr(IV) organoimido porphyrin complex, *p*-MeC$_6$H$_4$N═Cr(TPP) from the treatment of Cr(TPP) with excess *p*-tolyl azide in toluene.

Summary

The chromous dimer **1**$_2$ possesses a weak metal−metal interaction that enables it to behave as a source of **1** in the formation of simple adducts, **1**-L$_2$, a Cr(VI) dihydrazido species, species **2**, and Cr(IV) and Cr(VI) imido complexes, (^{t}Bu$_3$SiO)$_2$Cr(═NR)$_x$ (x = 1, **3**-R; 2, **4**-R).

Experimental Section

General Considerations. All manipulations were performed using either glovebox or high vacuum line techniques. Hydrocarbon solvents containing 1−2 mL of added tetraglyme and ethereal solvents were distilled under nitrogen from purple sodium benzophenone ketyl and vacuum-transferred from same prior to use. C$_6$D$_6$ was dried over activated 4 Å molecular sieves, vacuum transferred, and stored under N$_2$. The compounds CrCl$_2$(thf),[55] NaOSi^{t}Bu$_3$,[56] Ph$_2$CN$_2$,[57] and N$_3$R (R = Ad (adamantyl) 2,6-^{i}Pr$_2$-C$_6$H$_3$, 2,4,6-Me$_3$-C$_6$H$_2$ (Mes), 1-Naph (1-naphthalenyl), 2-Anth (2-anthracenyl),[58] and 2,6-Ph$_2$-C$_6$H$_3$)[59] were prepared according to literature procedures. All other chemicals were purchased from commercial sources and used as received. Benzophenone was purified by sublimation prior to usage. All glassware was oven-dried, and NMR tubes for sealed-tube experiments were additionally flame-dried under dynamic vacuum.

NMR spectra were obtained using INOVA-400 and Unity-500 spectrometers, and chemical shifts are reported relative to C$_6$D$_6$ (^{1}H, δ 7.15; ^{13}C{^{1}H}, δ 128.39). Infrared spectra were recorded on a Nicolet Impact 410 spectrophotometer interfaced to a Gateway

(39) Chisholm, M. H.; Folting, K.; Huffman, J. C.; Ratermann, A. L. *J. Chem. Soc., Chem. Commun.* **1981**, 1229−1230.
(40) Kool, L. B.; Rausch, M. D.; Alt, H. G.; Herberhold, M.; Hill, A. F.; Thewalt, U.; Wolf, B. *J. Chem. Soc., Chem. Commun.* **1986**, 408−409.
(41) Gerlach, C. P.; Arnold, J. *Organometallics* **1997**, *16*, 5148−5157.
(42) Chew, K. C.; Clegg, W.; Coles, M. P.; Elsegood, M. R. J.; Gibson, V. C.; White, A. J. P.; Williams, D. J. *J. Chem. Soc., Dalton. Trans.* **1999**, 2633−2639.
(43) Nugent, W. A.; Harlow, R. L. *Inorg. Chem.* **1980**, *19*, 777−779.
(44) Chiu, H. T.; Chen, Y. P.; Chuang, S. H.; Jen, J. S.; Lee, G. H.; Peng, S. M. *J. Chem. Soc., Chem. Commun.* **1996**, 139−140.
(45) Danopoulos, A. A.; Wilkinson, G.; Sweet, T. K. N.; Hursthouse, M. B. *J. Chem. Soc., Dalton. Trans.* **1995**, 2111−2123.
(46) Leung, W.-H. *Eur. J. Inorg. Chem.* **2003**, 583−593.
(47) Coles, M. P.; Dalby, C. I.; Gibson, V. C.; Clegg, W.; Elsegood, M. R. J. *J. Chem. Soc., Chem. Commun.* **1995**, 1709−1710.
(48) Danopoulos, A. A.; Hussain-Bates, B.; Hursthouse, M. B.; Leung, W.-H.; Wilkinson, G. *J. Chem. Soc., Chem. Commun.* **1990**, 1678−1679.
(49) Wiberg, N.; Häring, H. W.; Schubert, U. *Z. Naturforsch., Teil B* **1978**, *33*, 1365−1369.
(50) Danopoulos, A. A.; Leung, W. H.; Wilkinson, G.; Hussain-Bates, B.; Hursthouse, M. B. *Polyhedron* **1990**, *9*, 2625−2634.
(51) Eppley, D. F.; Wolczanski. P. T.; Van Duyne, G. D. *Angew. Chem., Int. Ed. Engl.* **1991**, *30*, 584−585.
(52) Soo, H. S.; Figueroa, J. S.; Cummins, C. C. *J. Am. Chem. Soc.* **2004**, *126*, 11370−11376.
(53) Barron, A. R.; Salt, J. E.; Wilkinson, G.; Motevalli, M.; Hursthouse, M. B. *J. Chem. Soc., Dalton. Trans.* **1987**, 2947−2954.
(54) Elliott, R. L.; Nichols, P. J.; West, B. O. *Polyhedron*, **1987**, *6*, 2191−2192.
(55) Kern, R. J. *Inorg. Nucl. Chem.* **1962**, *24*, 1105−1109.
(56) LaPointe, R. E.; Wolczanski, P. T.; Van Duyne, G. D. *Organometallics* **1985**, *4*, 1810−1818.
(57) Miller, J. B. *J. Org. Chem.* **1959**, *24*, 560−561.
(58) Liu, Q.; Tor, Y. *Org. Lett.* **2003**, *5*, 2571−2572.
(59) (a) Miura, Y.; Hiroyuki, O.; Momoki, M. *Synthesis* **1995**, *11*, 1419−1422. (b) Ozasa, S.; Fujioka, Y.; Ichiro, J.; Eiichi, K.; *Chem. Pharm. Bull.* **1983**, *31*, 1572−1581. (c) Gavenonis, J.; Tilley, T. D. *Organometallics* **2002**, *21*, 5549−5563

PC. Elemental analyses were performed by Oneida Research Services, Whitesboro, NY, or Robertson Microlit Laboratories, Madison, NJ. Magnetic moments were determined in C_6D_6 at room temperature using Evans' method[16] with an applied diamagnetic correction.

Procedures. 1. [(^{t}Bu$_3$SiO)Cr]$_2$(μ-OSi^{t}Bu$_3$)$_2$ (1$_2$). A 50 mL flask was charged with $CrCl_2$(thf) (0.600 g, 3.077 mmol), NaOSi^{t}Bu$_3$ (1.070 g, 4.487 mmol), and thf (40 mL). The mixture was stirred at 23 °C for 10 h, and the solvent was removed under vacuum. The green solid was heated at 70 °C under vacuum to effect desolvation, extracted with pentane, and filtered. The solution was concentrated and crystallized at −78 °C to yield **1**$_2$ as green blocks (0.806 g, 74% based on NaOSi^{t}Bu$_3$). ^{1}H NMR (C_6D_6, 400 MHz): δ 1.71 ($\nu_{1/2} \approx$ 210 Hz). IR (Nujol Mull, NaCl, cm^{-1}): 1012 (w), 952 (m), 922 (s), 858 (m), 820 (s), 621 (s). Anal. Calcd $C_{24}H_{54}Si_2O_2Cr$: C, 59.68; H, 11.29. Found: C 56.8, H 11.2. μ_{eff}(293 K) = 2.8 μ_B (Evans' method in C_6D_6).

2. *trans*-(^{t}Bu$_3$SiO)$_2$Cr(*p*-NCC$_6$H$_4$Me)$_2$ (1-(NCtol)$_2$). *p*-NCC$_6$H$_4$Me (0.049 g, 0.418 mmol) was added to a pentane solution of **1**$_2$ (0.100 g, 0.104 mmol)**.** Yellow crystalline **1**-(NCtol)$_2$ precipitated over 20 min (0.138 g, 93%). ^{1}H NMR (C_6D_6, 400 MHz): δ −13.04 ($\nu_{1/2} \approx$ 470 Hz, 4H, CH), 3.35 ($\nu_{1/2} \approx$ 800 Hz, 54H, silox), 16.11 ($\nu_{1/2} \approx$ 100 Hz, 4H, CH), 20.97 ($\nu_{1/2} \approx$ 110 Hz, 6H, Me). IR (Nujol Mull, NaCl, cm^{-1}): 2258 (s), 1606 (s), 1509 (m), 1178 (m), 997 (br s), 933 (w), 816 (s), 614 (s), 552 (s). Anal. Calcd $C_{40}H_{68}Si_2N_2O_2Cr$: C, 64.6; H, 10.3; N, 4.2. Found: C, 61.8; H, 9.4; N, 5.5. μ_{eff}(293 K) = 4.8 μ_B (Evans' method in C_6D_6).

3. *trans*-(^{t}Bu$_3$SiO)$_2$Cr(NC^{t}Bu)$_2$ (1-(NC^{t}Bu)$_2$). ^{t}BuCN (9 μL, 0.08 mmol) was added to a C_6D_6 solution containing **1**$_2$ (0.020 g, 0.0207 mmol). The solution turned pink instantaneously. Slow evaporation of the C_6D_6 solution yielded pink solid **1**-(NC^{t}Bu)$_2$ (∼0.015 g, ∼60%). ^{1}H NMR (C_6D_6, 400 MHz): δ 3.04 ($\nu_{1/2} \approx$ 670 Hz, 54H, C(CH$_3$)$_3$), 5.73 ($\nu_{1/2} \approx$ 230 Hz, 18H, NC^{t}Bu). IR (Nujol Mull, NaCl, cm^{-1}): 2272 (s), 1239 (m), 1207 (w), 1027 (s), 986 (s), 932 (m), 817 (m), 614 (s), 583 (m).

4. *trans*-(^{t}Bu$_3$SiO)$_2$Cr(CN^{t}Bu)$_2$ (1-(CN^{t}Bu)$_2$). A 3 dram vial was charged with **1**$_2$ (0.101 g, 0.105 mmol), CN^{t}Bu (47 μL, 0.449 mmol), and pentane (3 mL). The solution was allowed to sit 16 h, and then the solvent was allowed to slowly evaporate at 23°C to yield orange microcrystalline **1**-(CN^{t}Bu)$_2$ (0.113 g, 83%). ^{1}H NMR (C_6D_6, 300 MHz): δ 3.17 (peak has an upfield shoulder, $\nu_{1/2} \approx$ 700 Hz). IR (Nujol Mull, NaCl, cm^{-1}): 2192 (s), 2099 (m), 1237 (m), 1206 (s), 1024 (s), 977 (s), 851 (w), 817 (s), 707 (w), 615 (s). μ_{eff}(293 K) = 4.8 μ_B (Evans' method in C_6D_6).

5. (^{t}Bu$_3$SiO)$_2$Cr(PMe$_3$)$_2$ (1-(PMe$_3$)$_2$). An NMR tube was charged with **1**$_2$ (0.025 g, 0.0518 mmol) and PMe$_3$ (0.5 mL), forming a deep blue solution. The PMe$_3$ was removed under vacuum to yield a tacky blue solid. Attempts at scaling up the reaction resulted in deep blue oils. ^{1}H NMR (C_6D_6, 400 MHz): δ 1.23 ($\nu_{1/2} \approx$ 680 Hz, 54H, C(CH$_3$)$_3$), 17.79 ($\nu_{1/2} \approx$ 900 Hz, 18H, PMe$_3$).

6. *trans*-(^{t}Bu$_3$SiO)$_2$Cr(O=CPh$_2$)$_2$ (1-(OCPh$_2$)$_2$). A 3 dram vial was charged with **1**$_2$ (0.080 g, 0.083 mmol), benzophenone (0.060 g, 0.329 mmol), and heptane (2 mL). The solution was allowed to sit 16 h, and then the solvent was allowed to slowly evaporate at 23 °C to yield purple-red microcrystalline **1**-(OCPh$_2$)$_2$ (0.092 g, 66%). ^{1}H NMR (C_6D_6, 400 MHz): δ 1.72, 3.21 (resonances overlap). IR (Nujol Mull, NaCl, cm^{-1}): 1625 (s), 1598 (s), 1574 (s), 1329 (s), 1298 (s), 1285 (s), 1182 (m), 1160 (m), 989 (s), 948 (m), 940 (m), 928 (m), 819 (s), 766 (s), 709 (s), 696 (s), 643 (s), 616 (s). Anal. Calcd $C_{50}H_{74}Si_2O_4Cr$: C, 70.9; H, 8.8. Found: C, 69.2; H, 9.0. μ_{eff}(293 K) = 4.8 μ_B (Evans' method in C_6D_6).

7. 2. (^{t}Bu$_3$SiO)$_2$Cr(N$_2$CPh$_2$)$_2$ (2). A 4 dram vial was charged with **1**$_2$ (0.127 g, 0.132 mmol) and pentane (3 mL). Ph_2CN_2 (0.102 g, 0.525 mmol) was added to the green solution which instantly turned dark brown. The solution was allowed to slowly evaporate at −30 °C, yielding black crystals (0.129 g, 56%). ^{1}H NMR (C_6D_6, 400 MHz): δ 1.26 (s, 54H, C(CH$_3$)$_3$), 6.9−7.1 (m, 12H, CH$_{meta}$,-CH$_{para}$), 7.69 (d, ^3J = 5, 4H, CH$_{ortho}$). ^{13}C{^{1}H} NMR (C_6D_6, 400 MHz): δ 24.73, 30.89, 128.99, 131.10, 136.01, 149.95. IR (Nujol Mull, NaCl, cm^{-1}): 1587 (s), 1565 (s), 1321 (s), 1178 (m), 1077 (m), 1027 (m), 1000 (m), 983 (m), 956 (s), 933 (s), 909 (s), 818 (s), 775 (s), 765 (s), 693 (s), 655 (m), 622 (m), 570 (m). Anal. Calcd $C_{50}H_{74}Si_2N_4O_2Cr$: C, 68.9; H, 8.6; N, 6.4. Found: C, 68.8; H, 9.2; N, 4.8.

8. (^{t}Bu$_3$SiO)$_2$Cr=NAd (3-Ad). A 4 dram vial was charged with **1**$_2$ (0.080 g, 0.083 mmol), AdN_3 (0.029 g, 0.164 mmol), and pentane (3 mL). The solution was allowed to sit 12 h, and then the solvent was allowed to slowly evaporate at −30 °F to yield red microcrystalline **3**-Ad (0.071 g, 68%). ^{1}H NMR (C_6D_6, 400 MHz): δ −12.71 ($\nu_{1/2} \approx$ 380 Hz, 6H, CH$_2$), 2.05 ($\nu_{1/2} \approx$ 450 Hz, 54H, C(CH$_3$)$_3$), 4.28 ($\nu_{1/2} \approx$ 100 Hz, 6H, CH$_2$). IR (Nujol Mull, NaCl, cm^{-1}): 1306 (s), 1174 (m), 1150 (s), 1098 (s), 1084 (m), 1061 (s), 1027 (s), 986 (s), 944 (s), 901 (s), 858 (s), 816 (s), 709 (m), 672 (m), 619 (s). Anal. Calcd $C_{34}H_{69}Si_2NO_2Cr$: C, 64.6; H, 11.0; N, 2.2. Found: C, 64.2; H, 11.8; N, 2.8.

9. (silox)$_2$Cr=N(2,6-Ph$_2$C$_6$H$_3$) (3-(2,6-Ph$_2$-C$_6$H$_3$)). A 50 mL flask equipped with a stir bar was charged with **1**$_2$ (714 mg, 0.737 mmol), N$_3$(2,6-Ph$_2$)C$_6$H$_3$ (400 mg, 1.47 mmol), and 15 mL of pentane. Upon warming to 23 °C, the reaction mixture bubbled vigorously and turned reddish-brown. After the solution was stirred for 10 h at 23 °C, the volatile materials were removed, resulting in 932 mg of a red-brown **3**-(2,6-Ph$_2$-C$_6$H$_3$) (87%). ^{1}H NMR (C_6D_6, 400 MHz): δ −64.92 ($\upsilon_{1/2} \approx$ 90 Hz, 2H), −0.15 ($\upsilon_{1/2} \approx$ 40 Hz, 4H), 3.04 ($\upsilon_{1/2} \approx$ 140 Hz, 54H, C(C*H*$_3$)$_3$), 14.06 ($\upsilon_{1/2} \approx$ 20 Hz, 2H), 25.46 ($\upsilon_{1/2} \approx$ 210 Hz, 4H), 83.54 ($\upsilon_{1/2} \approx$ 80 Hz, 1H). IR (Nujol Mull, NaCl, cm^{-1}): 1500, 1295, 1116, 1096, 1067, 983, 817, 758, 698, 619. Anal. Calcd $CrSi_2O_2NC_{42}H_{67}$: C, 69.5; H, 9.3; N, 1.9. Found: C, 69.0; H, 9.6; N, 2.2. μ_{eff}(293 K) = 2.8 μ_B (Evans' method in C_6D_6).

10. (silox)$_2$Cr=N(2,6-^{i}Pr$_2$-C$_6$H$_3$) (3-(2,6-^{i}Pr$_2$-C$_6$H$_3$)). To separate 50 mL flasks on opposite ends of a double-ended frit fitted with a 90° needle valve was added **1**$_2$ (680 mg, 0.702 mmol) and N$_3$(2,6-^{i}Pr$_2$−C$_6$H$_3$) (285 mg, 1.40 mmol). Into the flask containing the azide was distilled 20 mL of pentane; the orange solution was then filtered to the flask containing **1**$_2$. Upon being mixed, effervescense and a color change to brown were noted. The solution was stirred for 10 h at 23 °C, and the volatile materials were removed, resulting in 758 mg of a dark brown **3**-(2,6-^{i}Pr$_2$-C$_6$H$_3$) (82% yield). ^{1}H NMR (C_6D_6, 500 MHz): δ −62.80 ($\upsilon_{1/2} \approx$ 135 Hz, 2H), −27.90 ($\upsilon_{1/2} \approx$ 550 Hz, 1H), 0.60 ($\upsilon_{1/2} \approx$ 160 Hz, 12H, CH(C*H*$_3$)$_2$), 3.56 ($\upsilon_{1/2} \approx$ 200 Hz, 54H, C(C*H*$_3$)$_3$), 93.40 ($\upsilon_{1/2} \approx$ 200 Hz, 2H) IR (Nujol Mull, NaCl, cm^{-1}): 1587, 1275, 1103, 1043, 817, 745, 618. Anal. Calcd $CrSi_2O_2NC_{36}H_{71}$: C, 65.7; H, 10.9; N, 2.1. Found: C, 65.5; H, 10.6; N, 2.4. μ_{eff}(293 K) = 2.7 μ_B (Evans' method in C_6D_6).

11. (silox)$_2$Cr=N(2,4,6-Me$_3$C$_6$H$_2$) (3-Mes). To separate 50 mL flasks on opposite ends of a double-ended frit fitted with a 90° needle valve were added 600 mg (0.619 mmol) of [Cr$_2$] and 200 mg (1.24 mmol) of N$_3$C$_6$H$_3$-(CH$_3$)$_3$-2,4,6. Into the flask containing the azide was distilled 20 mL of pentane; the orange solution was then filtered to the flask containing the [Cr$_2$]. Upon mixing, effervescense and a color change to red-brown were noted. The solution was stirred for 10 h at 25 °C, the volatile materials were stripped, resulting in 688 mg of a dark brown solid (90% yield). ^{1}H NMR (C_6D_6, 500 MHz): δ −93.46 ($\upsilon_{1/2} \approx$ 330 Hz, 3H), −68.00 ($\upsilon_{1/2} \approx$ 200 Hz, 2H), −55.61 ($\upsilon_{1/2} \approx$ 605 Hz, 6H), 3.74 ($\upsilon_{1/2} \approx$

200 Hz, 54H). IR (Nujol Mull, NaCl, cm^{-1}): 1600, 1288, 884, 811, 718, 625. Anal. Calcd $CrSi_2O_2NC_{33}H_{65}$: C, 64.3; H, 10.6; N, 2.3. Found: C, 64.0; H, 10.5; N, 2.5. μ_{eff}(293 K) = 2.7 μ_B (Evans' method in C_6D_6).

12. (^{t}Bu$_3$SiO)$_2$Cr(=NAd)$_2$ (4-Ad). A 10 mm o.d. glass tube was charged with **1**$_2$ (0.050 g, 0.052 mmol), AdN_3 (0.036 g, 0.203 mmol), and 4 mL of pentane. The solution was degassed, sealed, and heated at 100 °C for 4 h. The brown solution was slowly evaporated at −30 °C to yield brown-black crystals of **4**-Ad (0.038 g, 47%). ^{1}H NMR (C_6D_6, 400 MHz): δ 1.38 (s, 54H, C(CH_3)$_3$), 1.43 (br d, ^2J = 12 Hz, 6H, C^{4}H*H*), 1.52 (br d, ^2J = 12 Hz, 6H, C^4*H*H), 1.97 (br s, 6H, C^{3}H), 2.27 (d, ^3J = 3 Hz, 12H, C^{2}H$_2$). ^{13}C{^{1}H} NMR (C_6D_6, 400 MHz): δ 25.11 (*C*Me$_3$), 30.41 (C^{4}H$_2$), 31.21 (C(*C*H$_3$)$_3$), 36.49 (C^{2}H$_2$), 45.40 (CH), 82.23 (CN). IR (Nujol Mull, NaCl, cm^{-1}): 1298 (m), 1180 (m), 1163 (m), 1098 (m), 1028 (m), 974 (s), 913 (s), 819 (s), 622 (s). Anal. Calcd $C_{44}H_{84}Si_2N_2O_2Cr$: C, 67.6; H, 10.9; N, 3.6. Found: C, 66.4; H, 11.7; N, 3.6.

13. (silox)$_2$Cr(=N(1-Naph))$_2$ (4-1-Naph). A 1 dram vial was charged with 50 mg (0.052 mmol) of **1**$_2$ and 18 mg (0.105 mmol) of 1-azidonaphthalene. Upon introduction of 0.75 mL of C_6D_6, vigorous bubbling occurred and the solution turned dark brown. The solution was transferred to a J-Young tube, degassed, and allowed to sit for 10 h at 23 °C. Subsequent NMR analysis revealed **1**$_2$ and **4**-1-naph in a 1:2 ratio. ^{1}H NMR (C_6D_6, 300 MHz): δ 1.34 (s, 27H, C(CH_3)$_3$), 6.95 (m, 1H), 7.31 (m, 2H), 7.37 (s, 1H), 7.40 (s,1H), 7.99 (d, 1H), 8.84 (d, 1H).

14. (silox)$_2$Cr(=N(2-Anth))$_2$ (4-2-Anth). A 1 dram vial was charged with 41 mg (0.042 mmol) of **1**$_2$ and 19 mg (0.085 mmol) of 2-azidoanthracene. Upon introduction of 0.75 mL of C_6D_6, vigorous bubbling and a dark brown color were observed. The solution was transferred to a J-Young tube, degassed, and allowed to sit for 10 h at 23 °C. Subsequent NMR analysis revealed **1**$_2$ and **4**-2-Anth a 1:2 ratio. ^{1}H NMR (C_6D_6, 300 MHz): δ 1.45 (s, 27H, C(CH_3)$_3$), 6.49 (d, 1H), 7.11 (d, 1H), 7.13 (d, 1H), 7.46 (d, 1H), 7.63 (dd, 1H), 7.72 (dd, 1H), 7.85 (s,1H), 7.86 (s, 1H), 8.02 (s, 1H).

X-ray Crystal Structure Determinations. 1. 1$_2$. Slow evaporation of a pentane solution yielded green blocklike crystals of **1**$_2$ suitable for X-ray analysis. One crystal of dimensions 0.4 × 0.2 × 0.05 mm^3 was selected, coated in polyisobutylene, and placed under a 173 K nitrogen stream on the goniometer head of a Siemens SMART CCD area detector system. Preliminary diffraction data revealed an orthorhombic crystal system. A hemisphere routine was used for data collection, and the data were subsequently processed with the Bruker SAINT program to yield 15 103 reflections of which 15 103 were symmetry independent (R_{int} = 0.0000). The space group was determined to be *Pna*2$_1$ with the asymmetric unit consisting of $C_{106}H_{240}O_8Si_8Cr_4$. No inversion centers were detected by careful visual inspection of the packing diagrams, and an attempt to solve the structure in the centrosymmetric space group *Pnma* was unsuccessful. The data were corrected for absorption with SADABS, and the structure was solved by direct methods, completed by subsequent difference Fourier syntheses and refined by full-matrix least-squares procedures (SHELXTL). All non-hydrogen atoms were refined with anisotropic displacement parameters, and hydrogen atoms were included at calculated positions. The large structure contains severely disordered pentane molecules and large thermal displacement parameters of the *tert*-butyl methyl carbons.

2. 1-(OCPh$_2$)$_2$. Slow evaporation of a heptane solution yielded red-purple crystals of **1**-(OCPh$_2$)$_2$ suitable for X-ray analysis. One crystal of dimensions 0.5 × 0.4 × 0.3 mm^3 was selected, coated in polyisobutylene, and placed under a 173 K nitrogen stream on the goniometer head of a Siemens SMART CCD area detector system. Preliminary diffraction data revealed a monoclinic crystal system. A hemisphere routine was used for data collection, and the data were subsequently processed with the Bruker SAINT program to yield 3945 reflections of which 3901 were symmetry independent (R_{int} = 0.0302). The space group was determined to be *C*2 with the asymmetric unit consisting of $C_{25}H_{37}O_2SiCr_{0.5}$. The data were corrected for absorption with SADABS, and the structure was solved by direct methods, completed by subsequent difference Fourier syntheses and refined by full-matrix least-squares procedures (SHELXTL). All non-hydrogen atoms were refined with anisotropic displacement parameters, and hydrogen atoms were included at calculated positions.

3. 2. Slow evaporation at −30 °C of a pentane solution of **2** yielded brown crystals suitable for X-ray analysis. One crystal of dimensions 0.35 × 0.3 × 0.25 mm^3 was selected, coated in polyisobutylene, and placed under a 173 K nitrogen stream on the goniometer head of a Siemens SMART CCD area detector system. Preliminary diffraction data revealed a monoclinic crystal system. A hemisphere routine was used for data collection, which was subsequently processed with the Bruker SAINT program to yield 16 179 reflections of which 9125 were symmetry independent (R_{int} = 0.0468). The space group was determined to be *Pc* with the asymmetric unit consisting of $C_{55}H_{86}N_4O_2Si_2Cr$. The data were corrected for absorption with SADABS. The structure was solved by direct methods, completed by subsequent difference Fourier syntheses and refined by full-matrix least-squares procedures (SHELXTL). All non-hydrogen atoms were refined with anisotropic displacement parameters, and hydrogen atoms were included at calculated positions.

4. 3-(2,6-Ph$_2$-C$_6$H$_3$). Slow evaporation at −30 °C from a concentrated pentane solution gave red-brown crystals of **3**-(2,6-Ph$_2$-C$_6$H$_3$) suitable for X-ray diffraction. A crystal was isolated, covered in polyisobutylene, and placed under a 173 K nitrogen stream on the goniometer head of a Siemens P4 SMART CCD area detector. Preliminary diffraction data revealed an orthorhombic crystal system. A hemisphere routine was used for data collection, which was subsequently processed with the Bruker SAINT program to yield 25 415 reflections of which 8358 were symmetry independent (R_{int} = 0.0331). The space group was determined to be $P2_12_12_1$ with the asymmetric unit consisting of $C_{55}H_{86}N_4O_2Si_2Cr$. The data were corrected for absorption with SADABS. The structure was solved by direct methods, completed by subsequent difference Fourier syntheses, and refined by full-matrix least-squares procedures (SHELXTL). All non-hydrogen atoms were refined with anisotropic displacement parameters and hydrogen atoms were included at calculated positions. The *tert*-butyl groups of one silox (Si1) were disordered, and each was treated as two units of half-occupancy.

Magnetism of 1$_2$. Magnetization of microcrystalline and powdered samples was recorded with a SQUID magnetometer (Quantum Design) at 10 kOe between 5 and 300 K. The value for the magnetic susceptibility was corrected for the underlying diamagnetic increment (χ_{dia} = 733 × 10^{-6} cm^3mol^{-1}) by using tabulated Pascal constants[17] and the effect of the blank sample holders (gelatine capsule/straw).

Calculations. All ab initio quantum calculations were carried out using the GAMESS package.[60] The calculations were applied to the **1′**$_2$ system (Figure 2) using the crystallographic coordinates

(60) Schmidt, M. W.; Baldridge, K. K.; Boatz, J. A.; Elbert, S. T.; Gordon, M. S.; Jensen, J. J.; Koseki, S.; Matsunaga, N.; Nguyen, K. A.; Su, S.; Windus, T. L.; Dupuis, M.; Montgomery, J. A. *J. Comput. Chem.* **1993**, *14*, 1347−1363.

of one of dimers of $\mathbf{1}_2$. The geometry of the model was modified slightly to yield C_{2v} symmetry to aid in the electronic structure analysis. Both MCSCF[61] and MRMP2[62] methods with two selections of basis sets were employed. First, the CEP-31G[63] effective core potential basis set on all atoms with polarization functions on oxygen atoms (Basis Set I) was employed. Second, the CEP-31G basis set with polarization f[64] and (n+1)p[65] functions on chromium and the 6-311G (d,p)[66] basis set on oxygen and hydrogen atoms (Basis Sets II) was employed to assess basis set effects. For **3″**-Ph, the geometries of the GS and ES were optimized starting from pseudo-trigonal geometries by using the hybrid B3LYP[67] density functional and the CEP-31G(d) basis set.

Acknowledgment. We thank the National Science Foundation (CHE-0415506 (P.T.W.) and CHE-0309811 (T.R.C.)) for financial support and Prof. Karsten Meyer and Ingrid Castro Rodriguez for their time and effort in obtaining SQUID data on $\mathbf{1}_2$.

Supporting Information Available: CIF files for $\mathbf{1}_2$, **1**-$(OCPh_2)_2$, **2**, and **3**-(2,6-Ph_2-C_6H_3). This material is available free of charge via the Internet at http://pubs.acs.org.

IC051481W

(61) (a) Werner, H. J. *Adv. Chem. Phys.* **1987**, *69*, 1−62. (b) Shepard, R. *Adv. Chem. Phys.* **1987**, *69*, 63−200.
(62) Hirao, K. *Chem. Phys. Lett.* **1993**, *201*, 59−66.
(63) (a) Stevens, W. J.; Basch, H.; Krauss, M. *J. Chem. Phys.* **1984**, *81*, 6026−6033. (b) Stevens, W. J.; Krauss, M.; Basch, H.; Jasien, P. G. *Can. J. Chem.* **1992**, *70*, 612−630. (c) Cundari, T. R.; Stevens, W. J. *J. Chem. Phys.* **1993**, *98*, 5555−5565.
(64) Frenking, G.; Ehlers, A. W.; Boehme, M.; Dapprich, S.; Gobbi, A.; Hoellwarth, A.; Jonas, V.; Koehler, K. F.; Stegmann, R.; Veldkamp, A. *Chem. Phys. Lett.* **1993**, *208*, 111−114.
(65) Couty, M.; Hall, M. B. *J. Comput. Chem.* **1996**, *17*, 1359−1370.
(66) Krishnan, R.; Binkley, J. S.; Seeger, R.; Pople, J. A. *J. Chem. Phys.* **1980**, *72*, 650−654.
(67) (a) Becke, A. D. *J. Chem. Phys.* **1993**, *98*, 1372−1377. (b) Lee, C.; Yang, W.; Parr, R. G. *Phys. Rev.* **1988**, *B37*, 785−789.